

Clasts derived from rhizocretions in shallow-marine Miocene clastic deposits of northern Hungary: an example of zombie biogenic structures

Alfred UCHMAN¹, *, Árpád DÁVID² and Rozália FODOR³

- ¹ Jagiellonian University, Faculty of Geography and Geology, Institute of Geological Sciences, Gronostajowa 3a, 30-387 Kraków, Poland; ORCID: 0000-0002-0591-777X
- ² University of Debrecen, Department of Mineralogy and Geology, H-4032 Egyetem tér 1., Debrecen, Hungary; ORCID: 0000-0001-9609-917X
- ³ Mátra Museum of the Hungarian Natural History Museum, H-3200, Gyöngyös, Kossuth u. 40, Hungary; ORCID: 0000-0001-6441-2782



Uchman, A., Dávid, Á., Fodor, R., 2023. Clasts derived from rhizocretions in shallow-marine Miocene clastic deposits of northern Hungary: an example of zombie structures. *Geological Quarterly*, 2023, 67: 4, doi: 10.7306/gq.1674

Associate Editor: Anna Wysocka

Disc- and cylindrical-shaped clasts of fine-grained calcareous and ferruginous rock, each with a central tunnel, occur in shallow marine brackish Miocene sandy deposits of the Egyházasgerge Formation in Hungary. Previously, these have been interpreted as enigmatic biogenic (?) structures. After field and laboratory examination and comparisons with sub-recent rhizoclasts in subsoils developed on Quaternary fine-grained deposits in SE Poland, they are re-interpreted as redeposited rhizocretions possibly washed out of the coeval continental deposits of the Salgótarján Lignite Formation. Most are fragmented and abraded. They are termed rhizoclasts and are presented as an example of zombie structures inherited from another environment where they played a different role. Such rhizoclasts can be considered as an indicator of the source of the clastic material transported from a vegetated landmass on which moderate or poorly drained soils develop and plant roots penetrate the fine-grained substrate. In such soils, iron was mobilized, then fixed by oxidation, as the water table and oxygen levels fluctuated.

Key words: redeposition, concretions, rhizocretions, palaeosols, clastic deposits, Neogene.

INTRODUCTION

It appears that not only fossils but also some biogenically-induced diagenetic structures in marine deposits can be redeposited and inherited from other environments, that are not necessarily coeval and similar. Rhizocretions, i.e. concretions formed around plant roots, a kind of rhizolith (Klappa, 1980), are an example of that. They can be found in marine deposits as clasts and may be present as atypical transformed forms, which can be puzzling for investigators. Such clasts have been described from Miocene shallow marine deposits in northern Hungary and considered as enigmatic litho- or bioclasts by Radócz (1977), but their true nature was not then recognized.

In this paper, the clasts described by Radócz (1977) are re-examined and re-interpreted following rediscovery of his material (now in the Mátra Museum of the Hungarian Natural His-

tory Museum in Gyöngyös, Hungary), and field and laboratory studies of new material collected from the type locality and two other exposures in the same formation. The clasts are called rhizoclasts (a new term). Their interpretation is supported by comparisons with some *in situ* rhizocretions formed in the subsoil of Quaternary continental settings in southeastern Poland.

GEOLOGICAL SETTING

The deposits studied are part of the infill of the Pannonian Basin, which developed during the Cenozoic as a part of the Paratethys sea, and overlies different units of the Carpathians, Alps and Dinarides (Fig. 1). In the example described here, the Neogene deposits (Fig. 2) occur at the foot of the Bükk Mountains, where the basement of the Pannonian Basin crops out. The Upper Paleozoic–Mesozoic basement belongs to the Bükk Unit being a part of the Pelso Composite Unit within the ALCAPA Mega-unit (Csonotos and Vörös, 2004; Less et al., 2005). The stratigraphy of the Miocene deposits at the eastern margin of the Nógrád and Borsod basins (parts of the Pannonian Basin) is shown in Figure 3.

* Corresponding author, e-mail: alfred.uchman@uj.edu.pl

Received: October 26, 2022; accepted: January 5, 2023; first published online: March 14, 2023

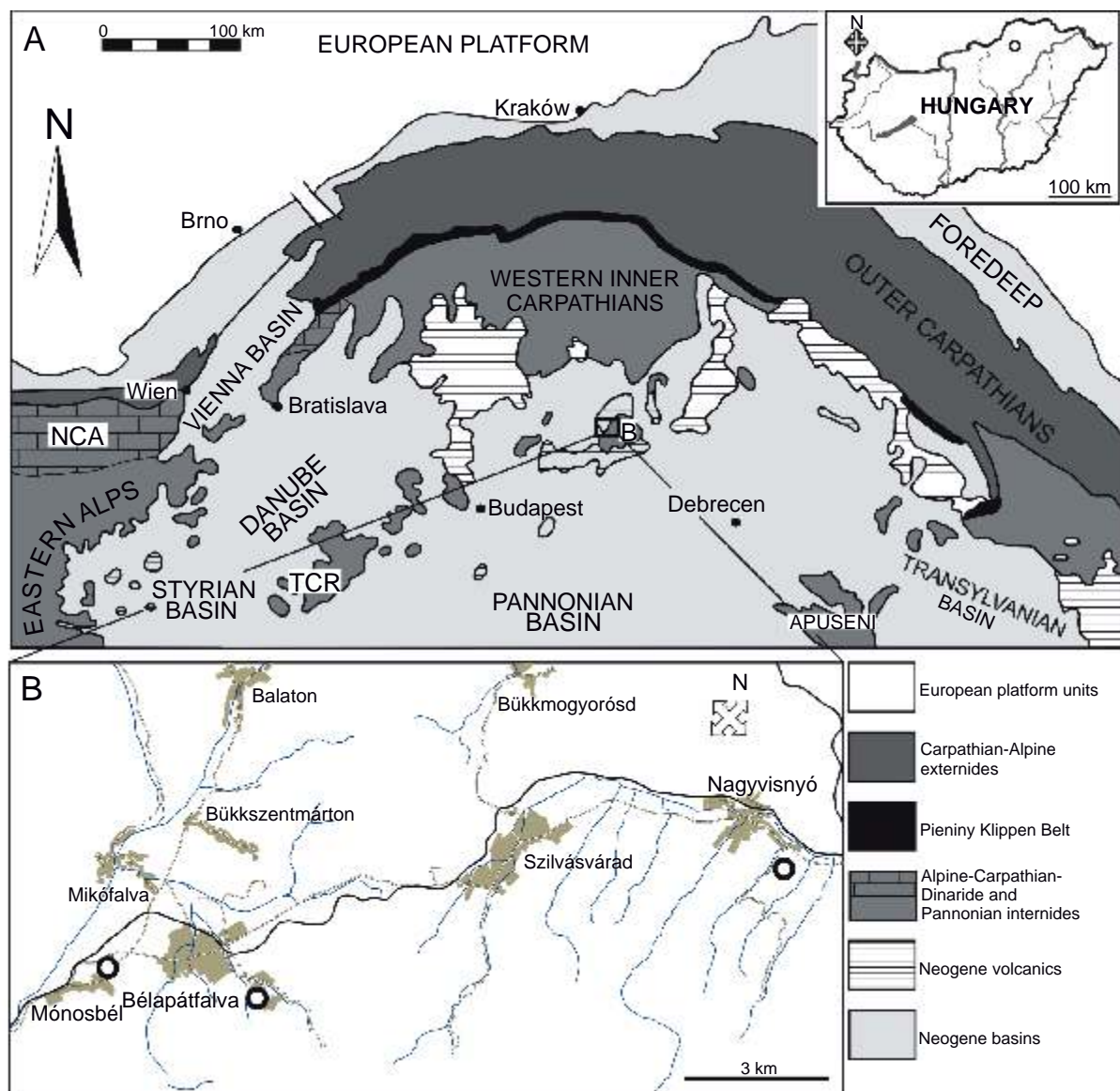


Fig. 1. Location maps

A – Western Carpathians region, showing the study area (**B**: based on Püspöki et al., 2017); in the corner, the map of Hungary showing the study area in the Bükk Mountains. NCA – Northern Calcareous Alps; TCR – Transdanubian Central Range; **B** – map of the localities studied

The deposits at the localities studied belong to the upper part of lower Miocene Egyházasgerge Formation, which typically starts with a basal conglomerate and continues with cross-bedded, *Chlamys*-bearing sand, sandstone, and gravel. These formed in a shoreline/nearshore environment. Locally, brackish-water estuarine deposits containing the bivalves *Congeria* and *Oncophora* (*Rzehakia*) are present and distinguished as the Kazar Sandstone Member. The Egyházasgerge Formation is 30–100 m thick. Its age is determined as Karpatian, which corresponds to the late Burdigalian (Less et al., 2005). The structures described occur in the marine parts of the formation, as inferred from body and trace fossils. The structures described here have been studied in at three localities (Figs. 4 and 5), which are abandoned sand pits, located in the western and northwestern part of the Bükk Mountains (Fig. 1).

The Nagyvisnyó (Lukács Hill) pit, located north-east of the village of Nagyvisnyó, on the southern flanks of Lukács Hill (48°08'19.30"N, 20°26'15.18"E), shows a profile, which begins with a 1 m thick, well-sorted, medium-grained, grey-coloured sand layer, which contains poorly preserved but abundant moulds of bivalves of the Cardidae forming a coquina (Figs. 4 and 5A). The grey sand is overlain by 4.5 m of fine-grained, limonitic sand. Both types of sand show trough cross-bedding, numerous clast horizons (including rhizoclasts; Fig. 5B, C), and six depositional units separated by erosional surfaces. The clasts often rest on these surfaces. 3D networks of *Ophiomorpha nodosa* penetrate the units from the erosional surfaces. Abundance of bioturbation structures fluctuates, decreasing downwards in the lowest 2 m of the unit, from BI = 3 to BI = 1 [using the bioturbation index (BI) of Taylor and Goldring, 1993].

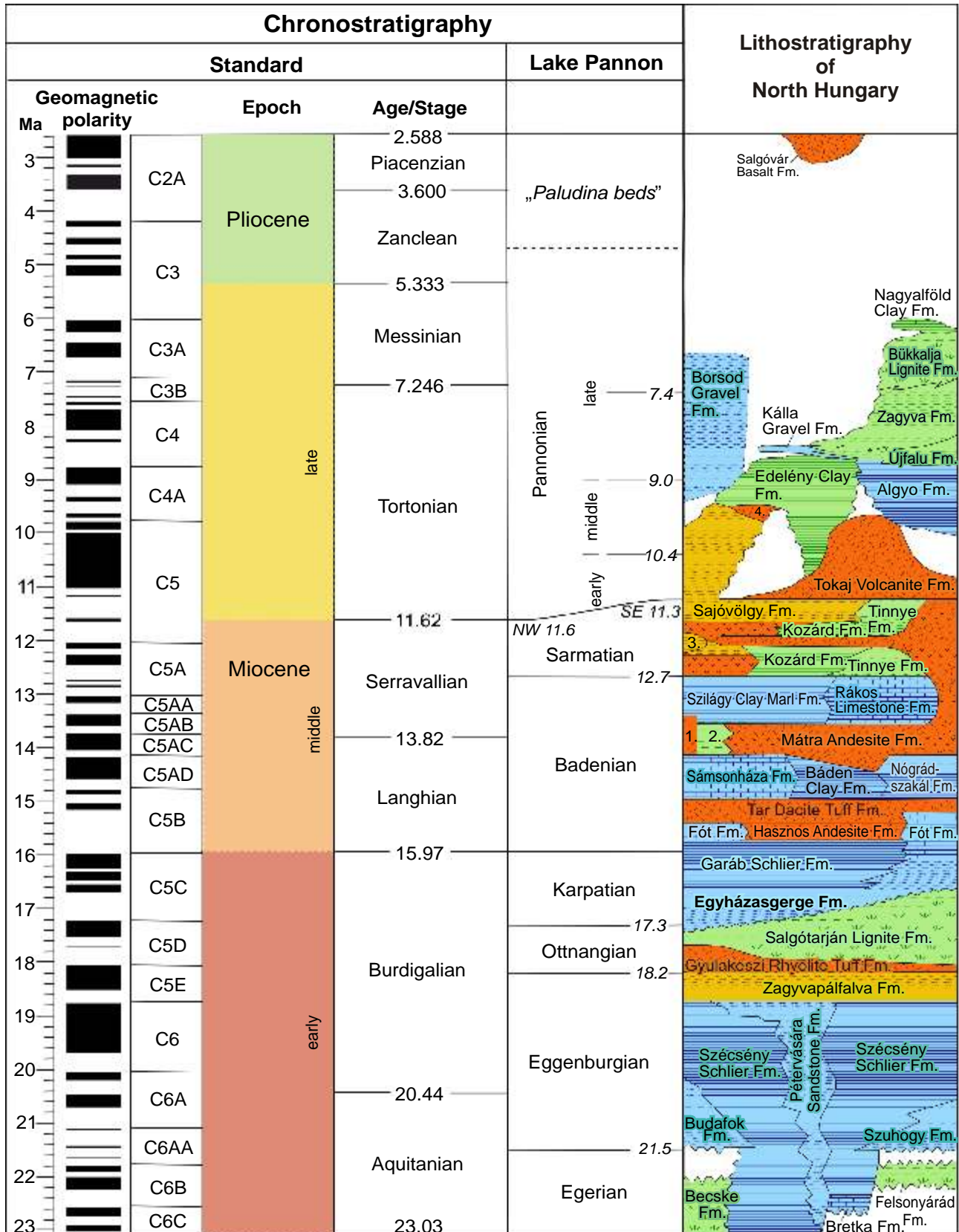


Fig. 2. Miocene stratigraphy of northern Hungary (based on Gyalog, 1996; Püspöki et al., 2017)

1 – Mátra Andesite Formation, 2 – Hidas Lignite Formation, 3 – Budajen Formation, 4 – Cserehát Rhyolite Tuff Formation

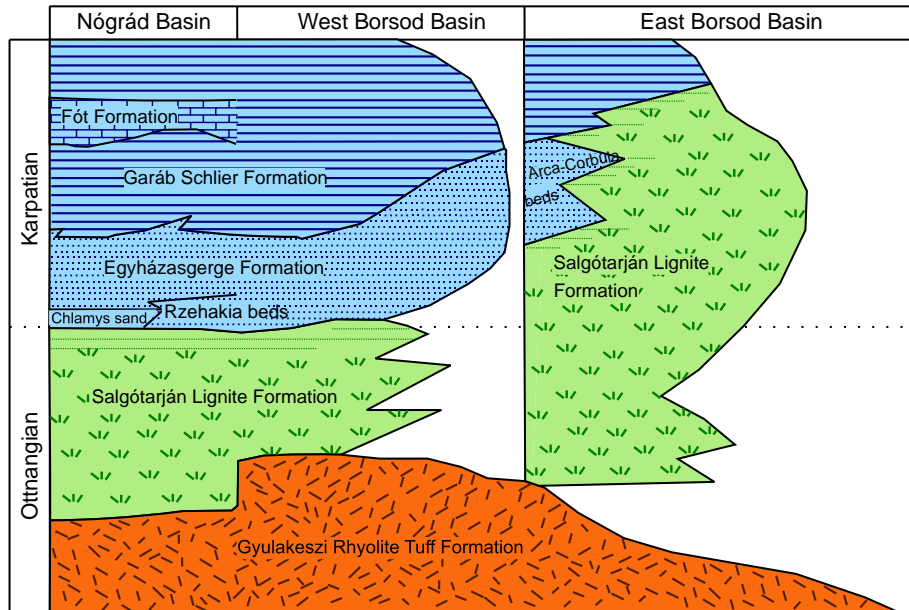


Fig. 3. Stratigraphy of the Ottnangian and the Karpatian in the area investigated (based on Gyalog, 1996; Püspöki et al., 2017)

A single specimen of *Gyrolithes nodosus* has also been observed. Characteristic macrofossils include Pectenidae valves and Balanidae tests (Dávid et al., 2008). The sand is overlain by a 0.5 m thick planar-laminated siltstone layer, which contains a few fragments of molluscan shells and is barren of bioturbation structures (Figs. 4 and 5A–C).

The Bélapátfalva pit (GPS coordinates: 48°03'14.88"N, 20°21'36.83"E) shows a 150 m-long exposure in the eastern part of the town of Bélapátfalva (Figs. 4 and 5D). The section is 16 m thick. The lowest 12 m comprises fine-grained, limonitic, calcareous, friable sandstone, with intercalations (15–20 cm thick) of calcium carbonate-cemented limonitic sandstone concretions. Numerous, nearly parallel clayey clast (including rhizoclast; Fig. 5E, F) horizons occur in friable sand. Limonitic impregnations mask the primary structures, but the clast horizons reveal very low-angle planar cross-stratification. Bioturbation structures are relatively rare. *Dactyloidites peniculus* has been observed at four levels (Dávid et al., 2015). Furthermore, *Ophiomorpha nodosa* occurs sporadically in the lower part. BI = 1 at these levels. The sand is overlain by 4 m of siltstone, which in its lower part contains a thin, planar parallel-laminated kaolinitic intercalation referred to as a volcanic ash fall. Some *Trichichnus*-like trace fossils can be observed in the middle and upper parts of the siltstone (BI = 1). Macrofossils have not been observed at this exposure (Figs. 4 and 5D–F).

The Mónosbél pit (GPS coordinates: 48°02'21.17"N, 20°20'12.71"E), in its lower part, shows 1.8 m of well-sorted, slightly limonitic, medium-grained sand with local thin intercalations of gravel and clay. The deposits are arranged into four sand bodies separated by erosional surfaces. The limonitic impregnations mask primary structures, but the clayey intercalations reveal low-angle planar cross-stratification. Mud clasts, rhizoclasts (Fig. 5G, H), and some pebbles are present in thin horizons concordant with sedimentary structures. The sandstones contain rare molluscan valve fragments and shark teeth. Bioturbation structures are limited to poorly preserved *Thalassinoides* (BI = 1), which is seen locally in cross-section in the lower-

most part. These deposits are overlain by a 5 cm thick fine-grained sand layer, which contains a few *Ostrea* valves, in turn capped by a 15 cm thick planar laminated siltstone followed by a 15 cm of planar-laminated clay; both are barren of bioturbation structures and macrofossils (Figs. 4 and 5G, H).

Additional material supporting interpretations provided in the Discussion derive from the Quaternary of SE Poland, where ferruginous rhizocretions were observed and collected at two localities, though much more can be found. The first locality is a forest road cut between Husów and Handzlówka (GPS coordinates: 49°59.693'N, 22°15.232'E) where Vistulian (Late Pleistocene) loess is exposed and is affected by pedogenesis in the upper part with podzolization (for loess in the region, see Laskowska-Wysoczańska, 1971). The second locality is in an abandoned (currently afforested) clay pit at Albigowa (GPS coordinates: 49°59.763'N, 22°11.449'E), where pedogenic processes developed on clays related to the middle Pleistocene Sanian Glaciation (Laskowska-Wysoczańska, 1995).

MATERIAL AND METHODS

A representative number of rhizoclasts have been collected, 51 from Nagyvisnyó, 101 from Bélapátfalva, and 24 from the Mónosbél pit. Furthermore, 222 rhizoclasts from the collection of Radóczy (1977) at the Mátra Museum of the Hungarian Natural History Museum in Gyöngyös, Hungary, were visually examined by hand lens and binocular microscope. Two thin sections of two spindle-shaped rhizoclasts from Bélapátfalva have been made, one along the long axis and one perpendicular to it. They were analysed and photographed under a *Nikkon Eclipse Ni* polarizing microscope, and by cathodoluminescence (CL) with a polarization light microscope (*Nikon Eclipse 50i*) and a Cambridge Image Technology (CITL) 8200 Mk three cold cathode set under standard carbonate operating conditions (electron beam voltage: ~12 kV, electric current: ~500 mA. A perpendicu-

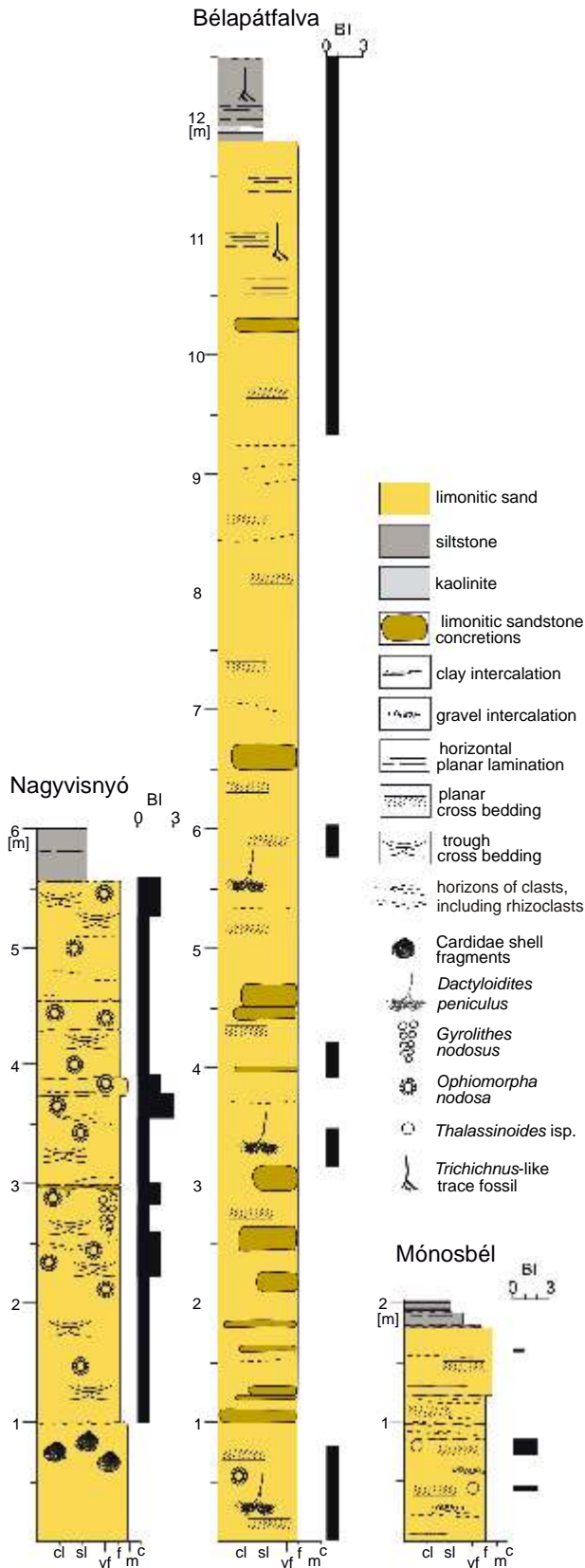


Fig. 4. Stratigraphic logs of the Egyházasgerge Formation (Miocene: Karpatian) in the exposures investigated

Grain-size scale: cl – clay, sl – silt, vf – very fine sand, f – fine sand, m – medium sand, c – coarse sand

lar broken surface of a spindle-shaped rhizoclast from Bélapátfalva was analysed using a *Rigoku SmartLa X-ray diffractometer*, and the *Scanning Electron Microscope* equipped with a *Hitachi 4700 EDS spectrometer*. The latest analysis (a perpendicular transect) was made on a thin-section of a rhizoclast from the same locality.

For comparison, comparable analysis of one thin-section was made using a polarizing microscope, and XRD, SEM, and EDS analyses of one rhizocretion were made, both from the Quaternary of SE Poland (the locality between Husów and Handzlówka: see Geological setting). All the instrumental analyses were carried out at the Jagiellonian University in Kraków, Poland.

MIOCENE RHIZOCLASTS AND QUATERNARY RHIZOCRETIONS

In the sections investigated, the rhizoclasts are dispersed in sand, or are aggregated in horizons. They show two basic morphotypes, i.e. 1) disc-shaped, pill-like rhizoclasts and 2) cylindrical rhizoclasts, as in the type material (Fig. 5).

The disc-shaped rhizoclasts are circular or regularly/irregularly elliptical in outline, 11–44 mm in diameter, 2–15 mm thick, with flat, slightly concave or slightly convex surfaces, rounded edges, with a central, more or less distinct pit or a hollow tunnel, which is perpendicular to the surfaces (Figs. 6A–C and 7). The pits or tunnels are circular or elliptical in outline, 1–4 mm wide. Some of them show a single concentric ring developed on 1) the same plane and bounded by a narrow furrow, or as 2) a low, flat elevation (Fig. 7L, N, Q). The ring may occupy a more central or a more external position. The surface of the discs is smooth (e.g., Figs. 6A, B and 7K), slightly corrugated (e.g., Fig. 7O, X), or covered by small, convex, concentrically arranged pads, mostly 1–3 mm wide (Fig. 7Y, Za). Some discs show short, cylindrical, or irregular bodies attached to their surface (Fig. 7D, V).

The cylindrical rhizoclasts are 15–85 mm long, up to 12–46 mm wide, circular to elliptical in transverse outline and spindle-, semi-spindle- or barrel-shaped in lateral outline (Figs. 6D, E and 8). They show a simple, centric or eccentric axial tunnel, straight or slightly winding, 1–3 mm wide, visible in the transverse section at the ends or partly on the abraded sides. The tunnel rarely branched and shows more frequent turns, as visible on broken surfaces (Fig. 8J). The tunnel is fully or partly filled. The infill may be missing at the terminations. Rarely, in abraded specimens, the tunnel is open along the whole length (Fig. 8A, R). The terminations of the rhizoclasts are blunt or broken along the transverse and oblique planes. Some specimens show a concentric structure. Rhizoclast surfaces are smooth or corrugated. Some specimens show indistinct transverse rings, which are occasionally highlighted by a change in colour (Fig. 8B, E, F). Both types of rhizoclast are mostly rusty brownish, less commonly brownish grey, yellowish, or creamy yellowish in colour.

One thin-section is oriented along the axial plane of a creamy yellowish to brownish cylindrical rhizoclast (Fig. 9A). Under binocular and polarizing microscope, it displays the axial zone, which is 6–8 mm wide. Its margins are uneven and diffuse. A 3 mm-wide axial tunnel runs along the centre of the axial zone and is filled with very fine silty calcium carbonate grains with dispersed, mostly

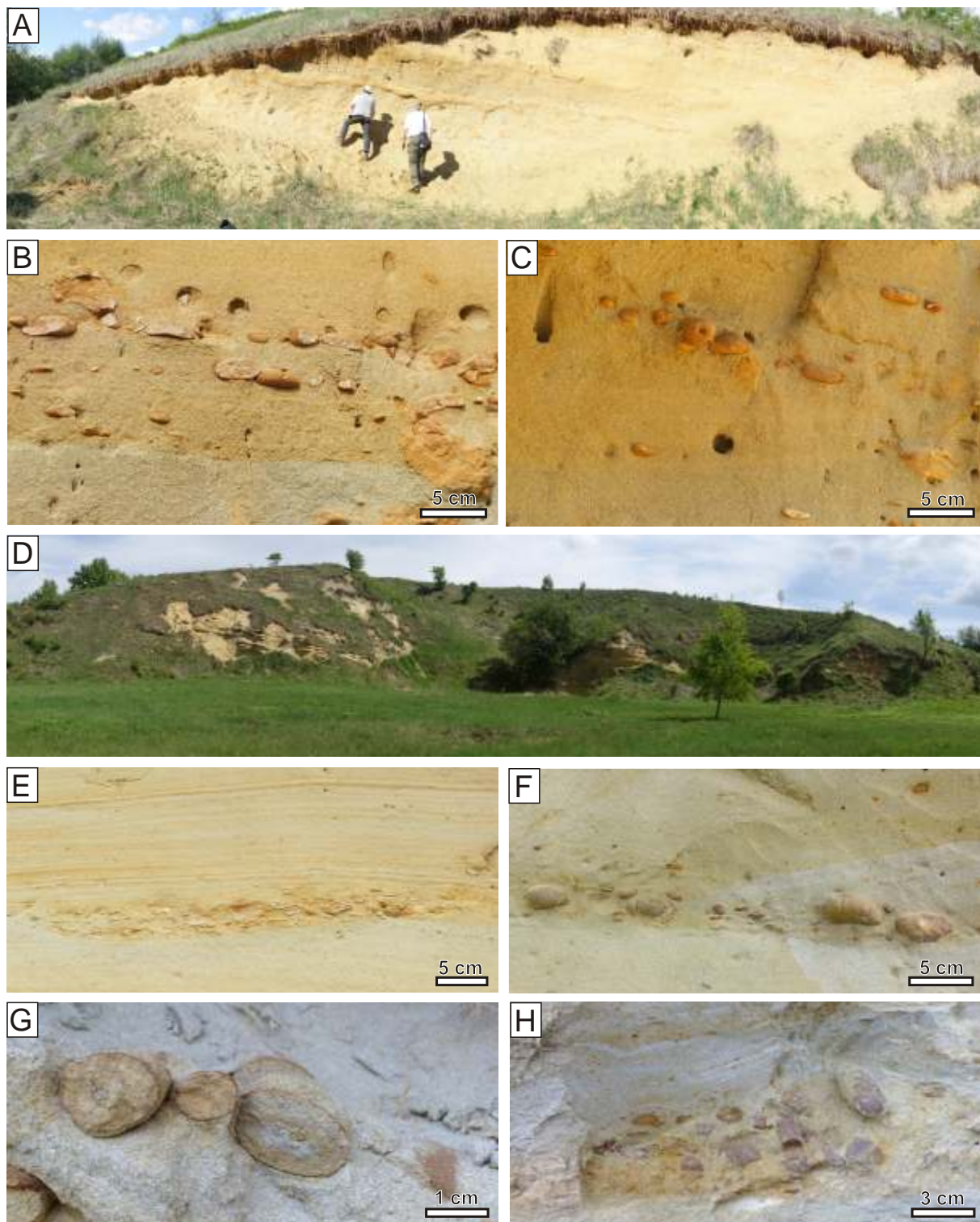


Fig. 5. View of the exposures and occurrences of the structures studied

A – exposure at Nagyvisnyó; **B, C** – studied rhizoclasts (some imbricated) within laminated sands (Nagyvisnyó section); **D** – exposures at Bélapátfalva; **E, F** – horizons with rhizoclasts in laminated sands in the Bélapátfalva section; **G** – cylindrical rhizoclasts in the Mónosbél section; **H** – oblique view of cylindrical rhizoclasts, which are aligned (Mónosbél section)

angular quartz grains and some ferruginous material. Here, this material and quartz grains are slightly more abundant than in the surrounding area. The material in the axial zone is coarser than in the axial tunnel and the external surroundings. The coarser material intrudes the external surroundings in triangu-

lar, outward-pointed (dental) enclaves. The body of the rhizoclast shows slightly oblique transverse zones, which are 4–7 mm wide, usually 2–3 mm apart, and run perpendicular from the axial zone to the margins of the rhizocretion. The transverse zones are paler than the surrounding areas, probably due

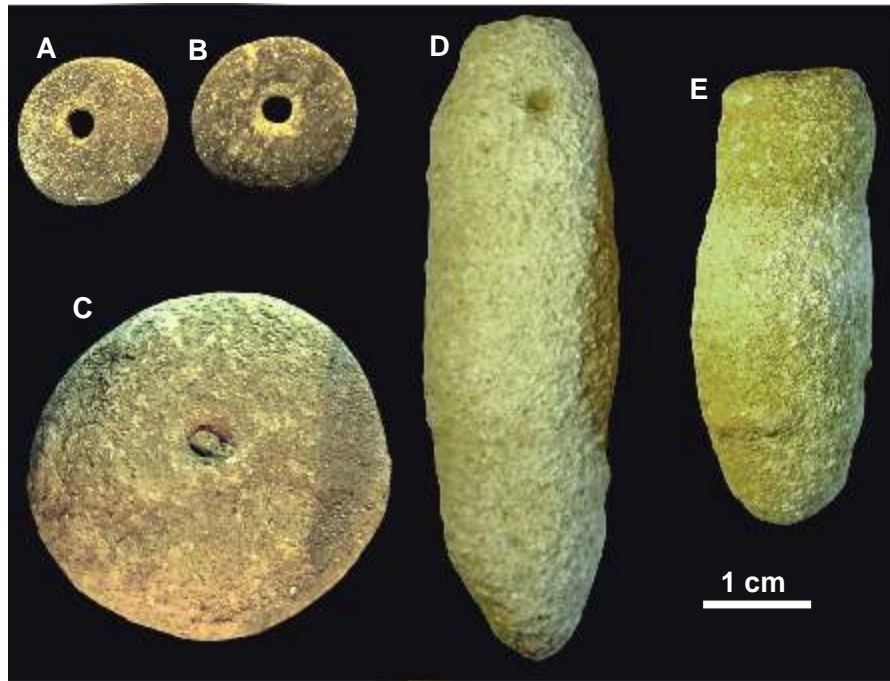


Fig. 6. Disk-shaped (A–C) and spindle-shaped (D, E) rhizoclasts from the material collected by Radóczy (1977) from the BÉlapátfalva sand pit

Mátra Museum of the Hungarian Natural History Museum in Gyöngyös, Hungary

to the higher content of the calcium carbonate grains. In addition to angular clastic grains (Fig. 9C–H), elliptical aggregations of calcium carbonate grains, 0.1–0.5 mm long, are visible (Fig. 9D, E, G, H). The margins of the aggregations range from even and regular to uneven and irregular in outline. Some of the angular clastic grains are unevenly coated with an almost black substance, which is probably iron or manganese oxides/oxyhydroxides (Fig. 9F).

Under the electron microscope and on the basis of EDS analysis, the thin-section described above shows mainly elongate calcite grains, which are mostly 20–30 μm in size, and have jagged margins (Fig. 10; Appendix 1). The space between the grains is porous, with some bridges between the grains (Fig. 10C, D), which are presumably cements. However, the crystals of the supposed cements cannot be seen under a polarizing microscope because they are too small. The porous space diminishes towards the axial zone (compare Fig. 10B versus Fig. 10E). The calcite grains form a matrix for larger silt or fine sand grains, usually angular, of quartz and dolomite or flakes of muscovite. These components are usually surrounded by pore space and “float” in the matrix. Moreover, small, irregular enclaves of iron oxyhydroxides, single grains of zircon, titanium oxides (probably rutile), and apatite were identified. Iron oxyhydroxides are more frequent in the marginal parts of the rhizoclast and in the axial zone (Fig. 10A, F).

The other thin-section runs perpendicular to a spindle-shaped rhizoclast (Fig. 9B). The composition observed under the polarizing microscope is the same as in the previous thin-section. Subtle changes in grain size and packing show a concentric pattern, which is elliptical in outline, developing around an elongated central slit with jagged margin. The slit is 3 mm long and up to 0.8 mm wide. Originally, it was filled with sandy material, coarser than in the body of the rhizoclasts, but this was removed during the production of the thin-section. Iron

oxyhydroxides are concentrated primarily at the margins. Very small oval or elongate aggregations of a brownish, non-transparent substance, presumably iron minerals, are present between the grains.

Only very few isolated carbonate grains from both thin-sections show rather poor luminescence. This prevented further investigations by cathodoluminescence.

Another spindle-shaped rhizoclast was analysed by means of an electron microscope and using EDS X-ray diffractometer analysis (Fig. 11, Appendix 2). This rhizoclast is deeply brownish-rusty in colour. In contrast to the previously described rhizoclasts observed in thin-sections, it is dominated by silt and very fine grains of quartz, iron oxyhydroxides and clay minerals. In addition, dolomite and feldspar grains and muscovite flakes are present. The overall content of calcium is subordinate. The composition is generally confirmed by the XRD analysis of a piece of this rhizoclast. This allowed identification of illite and kaolinite among clay minerals, plagioclase among feldspars, goethite among iron oxyhydroxides, and apatite (Appendix 4).

The Quaternary rhizocretions (Figs. 12 and 13) are generally spindle-shaped, non-calcareous, and rusty in colour. In microscopic view of a thin-section, they show silt-sized angular to sub-rounded quartz grains (dominant component), rare, dispersed muscovite flakes, other felsic grains, and an opaque ferruginous material. A millimetric, parallel or subparallel lamination is expressed by differences in contribution of the components (Fig. 14A, B). The electron microscope (Fig. 14C, D) and EDS analyses confirm this composition and reveal rare feldspar (including plagioclase) grains and the presence of manganese and titanium oxides (Appendix 3). This composition is also generally confirmed by the XRD analysis. In addition, this reveals a small amount of clay minerals, including chlorite and probably illite. Among the iron oxyhydroxides, lepidocrocite was identified (Appendix 4).

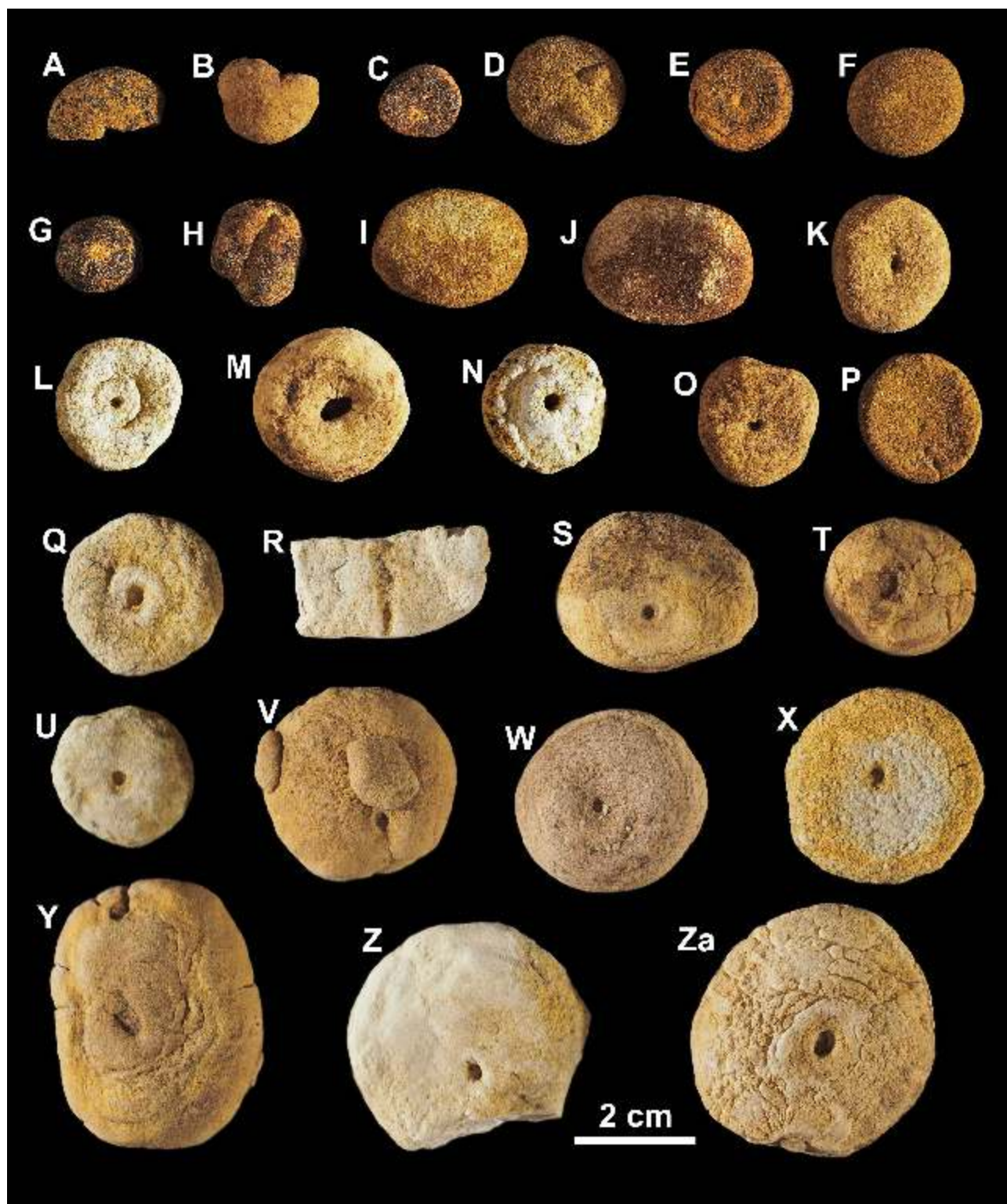


Fig. 7. Disc-shaped rhizoclasts

Specimens in Q, R, S, T, U, Y, V, W, Z, Za from the Nagyvisnyó section, and the remainder from the Mónosbél section;
 Nature Education Centre of the Jagiellonian University (CEP) – Museum of Geology, Kraków, Poland

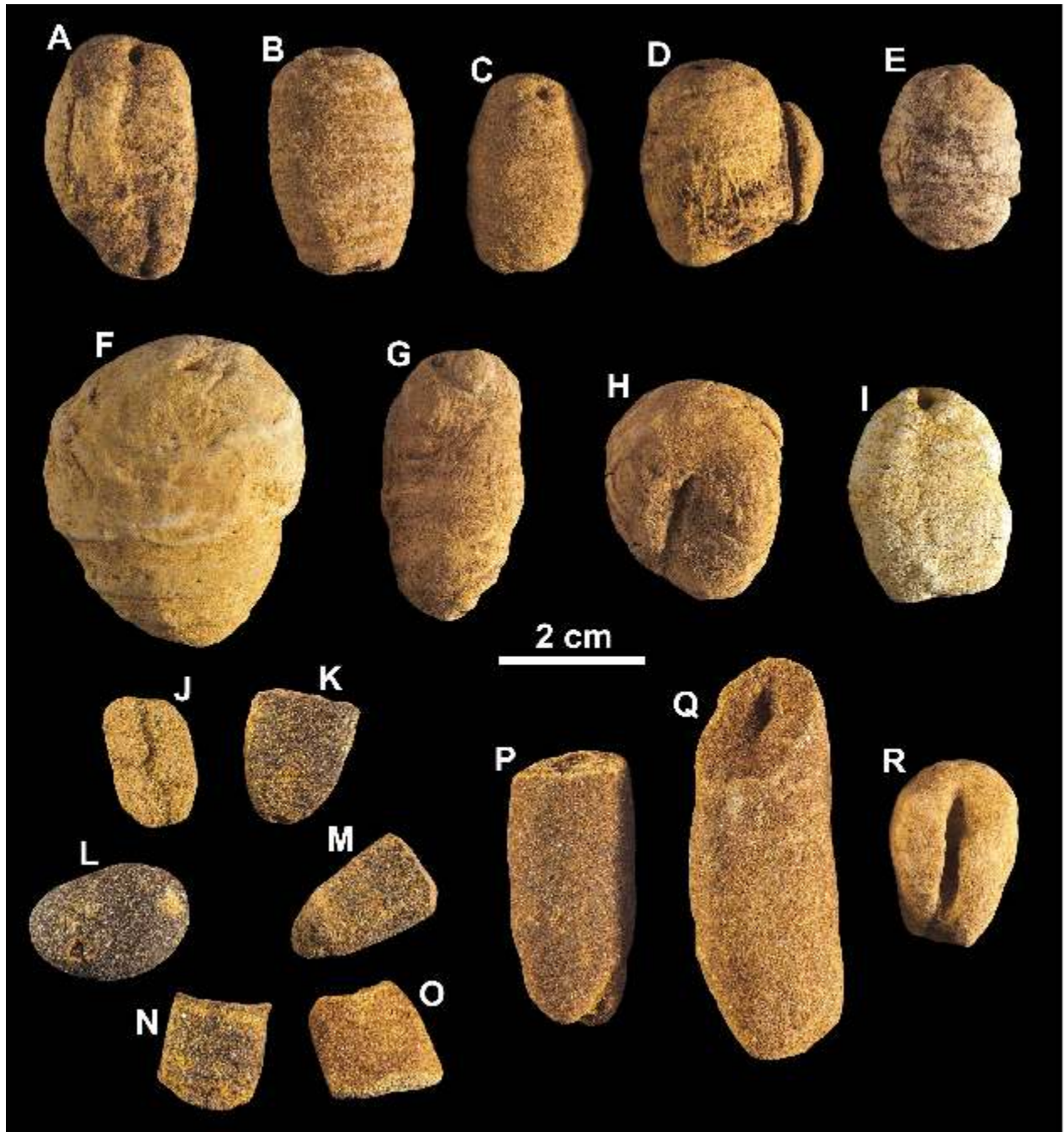


Fig. 8. Cylindrical (including spindle- and barrel-shaped) rhizoclasts

Specimens from 2A–I from the Nagyvisnyó section, and the remainder from the Mónosbél section; Nature Education Centre of the Jagiellonian University (CEP) – Museum of Geology, Kraków, Poland

DISCUSSION

NATURE OF THE RHIZOCLASTS

The rhizoclasts from the Bélapátfalva sand pit were described by Radócz (1977) (Fig. 6), who considered them as enigmatic trace fossils, which could be “internal moulds of various burrows”, coprolites in some cases, or “calcareous-limoni-

tic concretions or pseudomorphs left over by mud feeder worms or other skeletonless benthic forms”; however, he did not exclude inorganic origin for some of them. The main feature that puzzled Radócz was the axial tunnel.

This interpretation can be questioned on the basis of the material analysed herein, from the original locality and two additional localities of the same Miocene formation in Hungary (Figs. 6–9) and on the basis of reference material from the continental Quaternary of SE Poland. The nature of rhizocretions

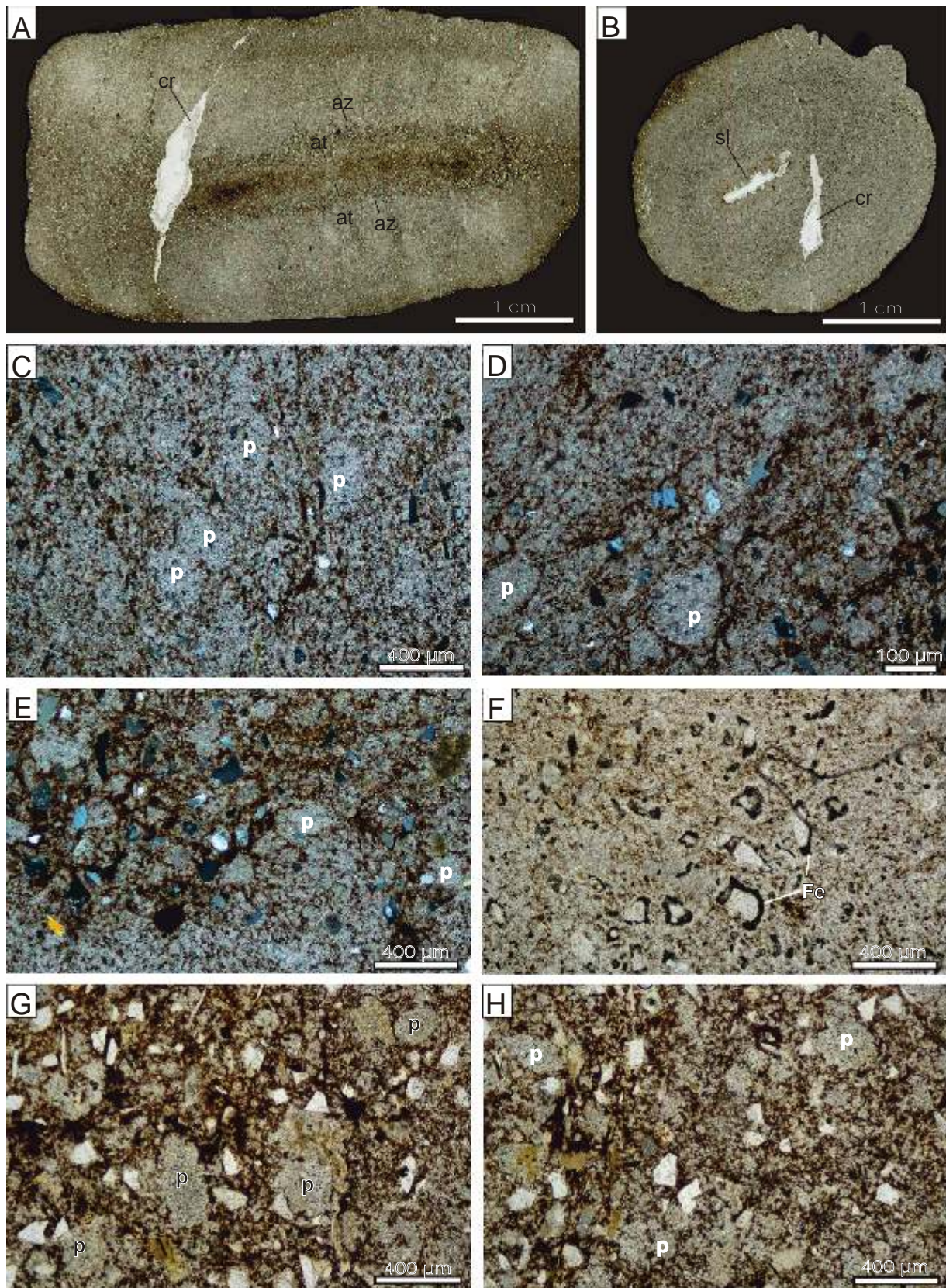


Fig. 9. Thin-sections of the cylindrical rhizoclasts

A – scan of a thin-section in the transverse plane; sl – slit with jagged margins, originally filled with sandy material; cr – crack of mechanical origin; **B** – scan of a thin-section in longitudinal, axial plane; at – axial tunnel; az – axial zone; cr – crack of mechanical origin; **C–H** – microphotographs of thin-sections; p – calcite-dominated elliptical aggregations, Fe – ferruginous coatings

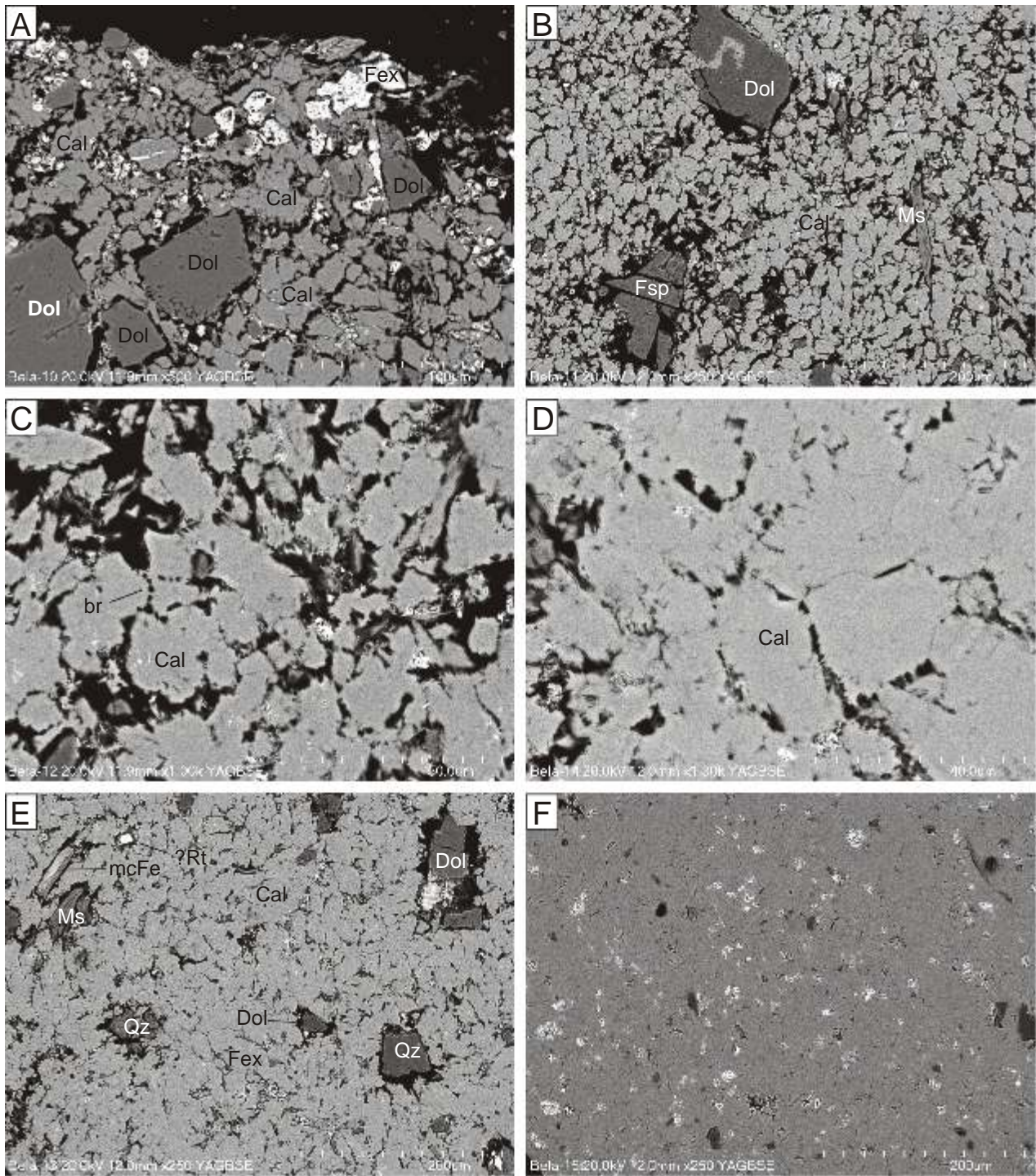


Fig. 10. Electron microscope images with identification of some minerals (Cal – calcite, Dol – dolomite, Fex – iron oxyhydroxides, Fsp – feldspar, mcFe – iron-rich mica, Ms – muscovite, Qz – quartz, ?Rt – titanium oxide, probably rutile) on the basis of EDS analysis of a thin-section oriented parallel to the axial zone of a spindle-shaped rhizoclast from the BÉlapátfalva pit

A–C – marginal part of the rhizoclast with black porous space between grains; **D–E** – more inner part of the rhizoclast with reduced black porous space between grains (br – an example of bridges between grains, probably cements); **F** – inner part of the rhizoclast; the pale enclaves are iron oxyhydroxides

from sub-recent subsoil developed on Quaternary deposits in SE Poland is obvious. At the first locality (see Geological setting), some of the rhizocretions have an elastic root inside, of a coniferous tree, the European silver fir *Abies alba*. Clearly, these are distributed around vertical or oblique segments, a few

centimetres long, of thin (up to a few millimetres) roots of ligneous and herbaceous plants. Therefore, it seems that at least some of them are still forming. At the second locality, the rhizocretions were vertically oriented but beyond the range of living roots. Such rhizocretions are known from other loess lo-

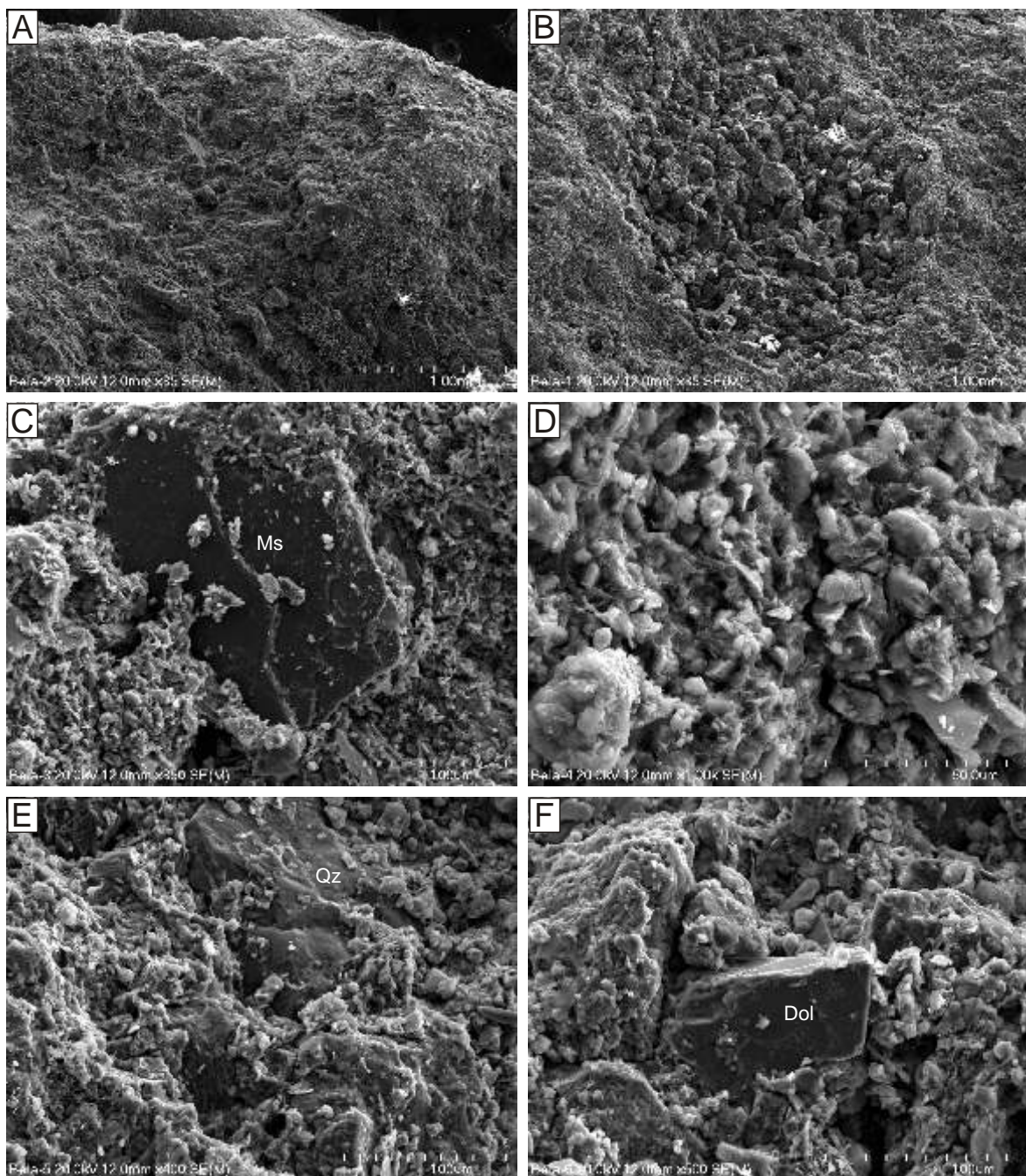


Fig. 11. SEM images of a transverse broken surface of a spindle-shaped rhizoclast, with identification of some minerals, on the basis of EDS analysis, from the BÉlapátfalva pit

A – marginal part of the rhizoclast; **B** – cross-section of the central tunnel filled with very fine quartz-dominated sand; **C** – muscovite flake (Ms) partially covered and surrounded by a mixture composed mainly of clay minerals and iron oxyhydroxides; **D** – a mixture composed mainly of clay minerals and iron oxyhydroxides; **E, F** – quartz (Qz) and dolomite (Dol) grains surround a mixture composed mainly of clay minerals and iron oxyhydroxides

calities (e.g., Klappa, 1980; Biernacka and Issmer, 1996; Becze-Deák et al., 1997; Łucka et al., 2008, 2009; Gocke et al., 2009, 2010, 2011; Barta, 2011) and other fine-grained deposits penetrated by roots (e.g., Sieglitz and Van Horn, 1982).

The shape and internal structure of the Quaternary rhizocretions at both localities in SE Poland (Figs. 12 and 13), as well as those described from the Quaternary of Japan (Yoshida et

al., 2008; Nanzyo and Kanno, 2018: fig. 5.6), display the same morphological principles and internal structure as the cylindrical rhizoclasts from the Miocene of Hungary. Therefore, the latter are interpreted as fragmented rhizocretions formed around plant roots in soil under terrestrial conditions.

The disc-shaped rhizoclasts have the same features as cylindrical rhizoclasts, except for extension along the axial tunnel.

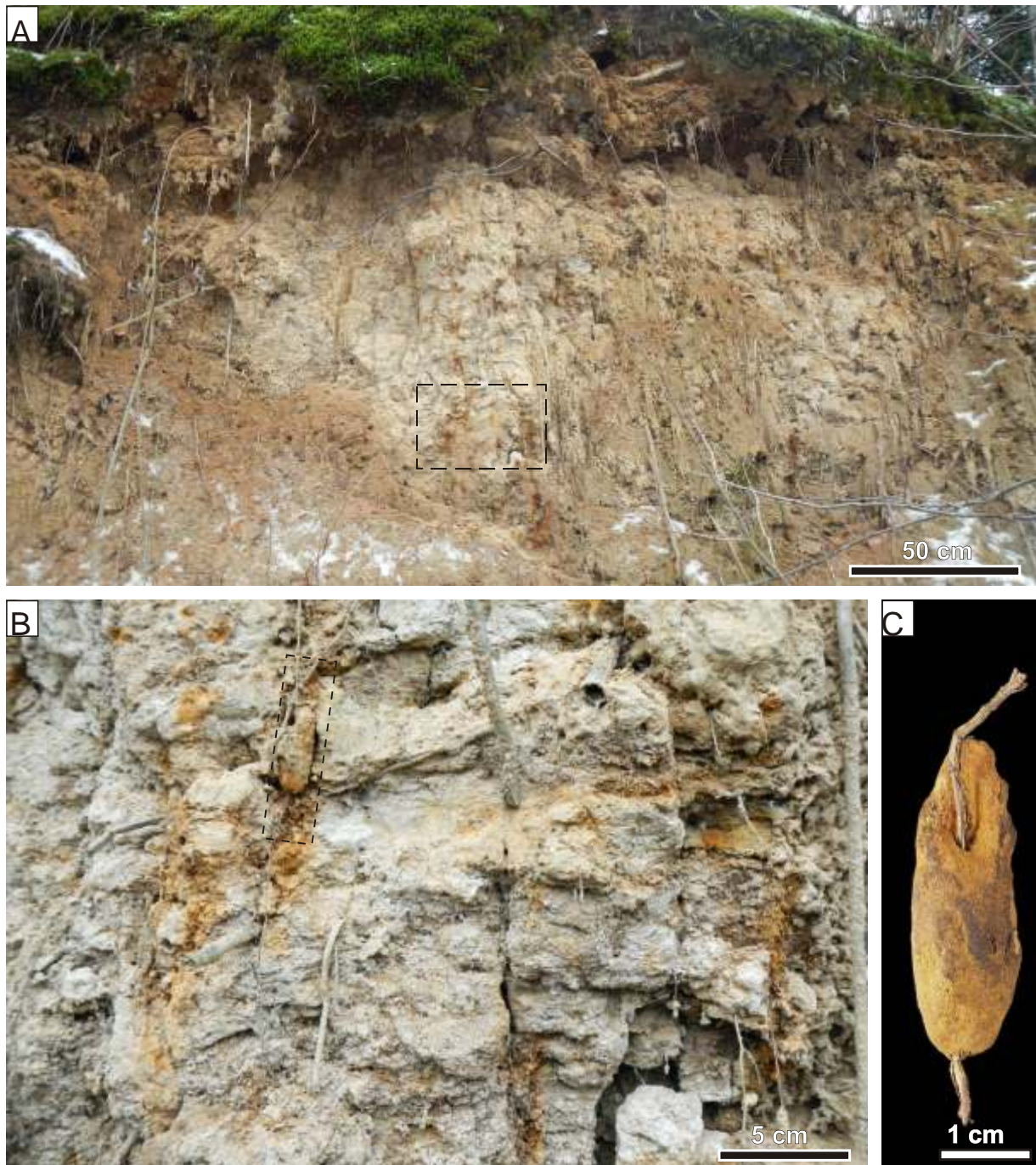


Fig. 12. Rhizcretions in Vistulian loess between Husów and Handzlówka, SE Poland

A – view of the exposure; close view in **B** indicated by the quadrangle; **B** – close view of **B**; several root zones are marked by ferruginization; rhizcretion illustrated in **C** indicated by the quadrangle;
C – rhizcretion exploited from the place indicated in **B**

These are considered as fragmented and abraded cylindrical rhizcretions (Fig. 15). The fragmentation of the cylindrical rhizcretions is enhanced by their internal lithological heterogeneity, which is visible as transverse zones (Fig. 8B) and manifested as rings on their surfaces (Fig. 8B, E, G).

Rhizcretions are usually the result of the precipitation of calcium carbonate, iron oxyhydroxides, or other iron minerals in the illuvial soil zone (cf. Sharkan and Achyuthan, 2007; Bojanowski et al., 2020). The axial tunnel is a trace of the root. In

some Quaternary rhizcretions, the plant root is still preserved (Fig. 12C), though usually the root has decomposed. The material surrounding the root is involved in the rhizcretion. Ferruginous concentrations around the central tunnel or on the surface are hypocoatings, typical of pedogenic processes (Chesworth, 2008; Vepreskas et al., 2018).

Calcium carbonate-rich crystal aggregations (Fig. 9D, E, G, H) may be interpreted as faecal pellets of some invertebrates. Carbonate faecal pellets are produced by earthworms (cf. Lee



Fig. 13. Rhizcretions from Vistulian clays in an abandoned clay pit at Albigowa, SE Poland

et al., 2008), and in smaller amounts by some slugs (Canti, 1998). Those produced by earthworms are called earthworm calcite granules. It is doubtful that the aggregations in the rhizoclasts described belong to them, as earthworm calcite granules usually have larger calcite crystals, greater than 0.05 mm (Durand et al., 2010). However, granules of some earthworm taxa contain smaller crystals (Canti and Pearce, 2003; Versteegh et al., 2013).

GENERAL REMARKS

The Miocene rhizcretions were exhumed from their original continental environment and involved in marine sedimentation, where they played a new role as rhizoclasts. Therefore, they are considered as zombie biogenic structures by analogy to zombie fossils (e.g., Archibald, 1996; Lane et al., 2005). It is

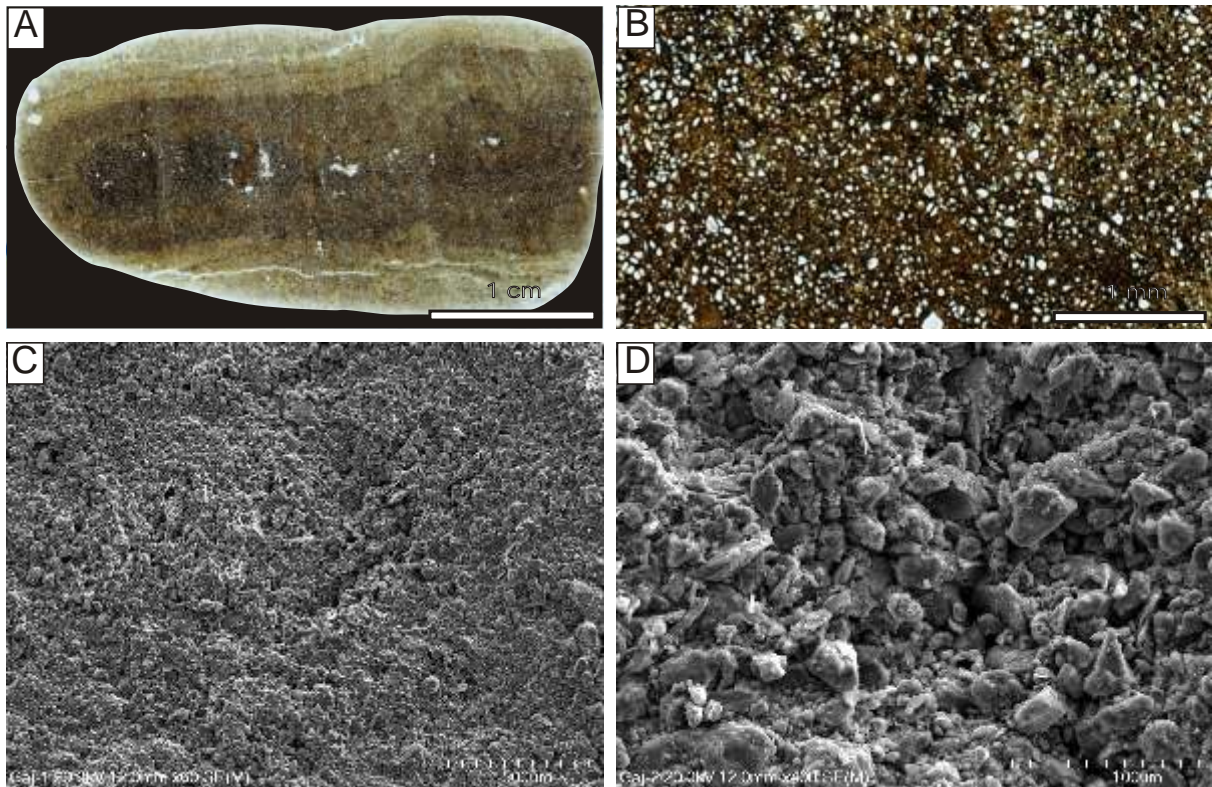


Fig. 14. Thin-section and SEM images of rhizocretions from Quaternary loess subsoil; locality between Husów and Handziłówka, SE Poland

possible that such structures are more common in similar deposits than previously thought, though usually overlooked or ignored. However, they can be a source of complementary information on the palaeoenvironment. Other examples of zombie biogenic structures come from some trace fossils, particularly *Ophiomorpha*, fragments of which can be redeposited as clasts (Löwemark et al., 2016; Pedrol de Freitas et al., 2020).

Redeposited rhizocretions/rhizoliths are very rarely recorded in the literature. Renaut (1993) and Owen et al. (2008) described redeposited rhizoliths that form thin beds cemented by calcite in Lake Bogoria in Kenya but these are not similar to those described here. Metodiev et al. (2022) reported some ferruginous nodules in shallow marine Middle Jurassic deposits in Bulgaria; they show a concentric inner structure and central tunnel and were interpreted as rhizocretions.

The presence of redeposited rhizoclasts in shallow-marine deposits of the Egyházasgerge Formation indicates erosion of vegetated soils on nearby land in which rhizocretions were forming. The soil developed on silty and very fine sandy substrate, as suggested by the material involved in the rhizocretions. The presence of both calcareous and ferruginous rhizoclasts at the same locality (Bélapátfalva), suggests derivation from different soils.

The disintegrated rhizocretions were transported as rhizoclasts by rivers, brought to the sea, and abraded along the way. The abrasion probably continued in the sea, as deposition took place within wave range. However, it is not excluded that the rhizocretions were eroded by the sea along the coast. A high-energy environment is indicated by preservation of cross-bedding with clast horizons, including of rhizoclasts, and the presence of the proximal *Cruziana* ichnofacies represented by

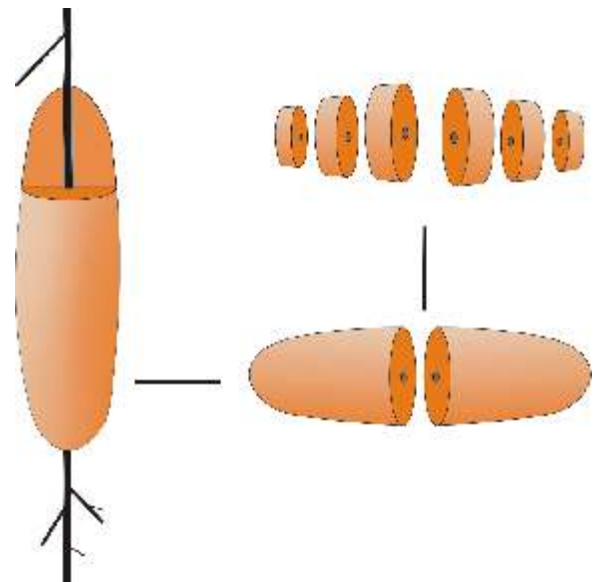


Fig. 15. Model of disintegration of a rhizocretion into fragments, which can then be redeposited as rhizoclasts

Ophiomorpha nodosa, *Dactyloidites peniculus* and *Thalassinoides*; the proximal *Cruziana* ichnofacies is typical mostly of the upper shoreface (Pemberton et al., 2001). However, the ichnofacies here is impoverished, probably because of lowered

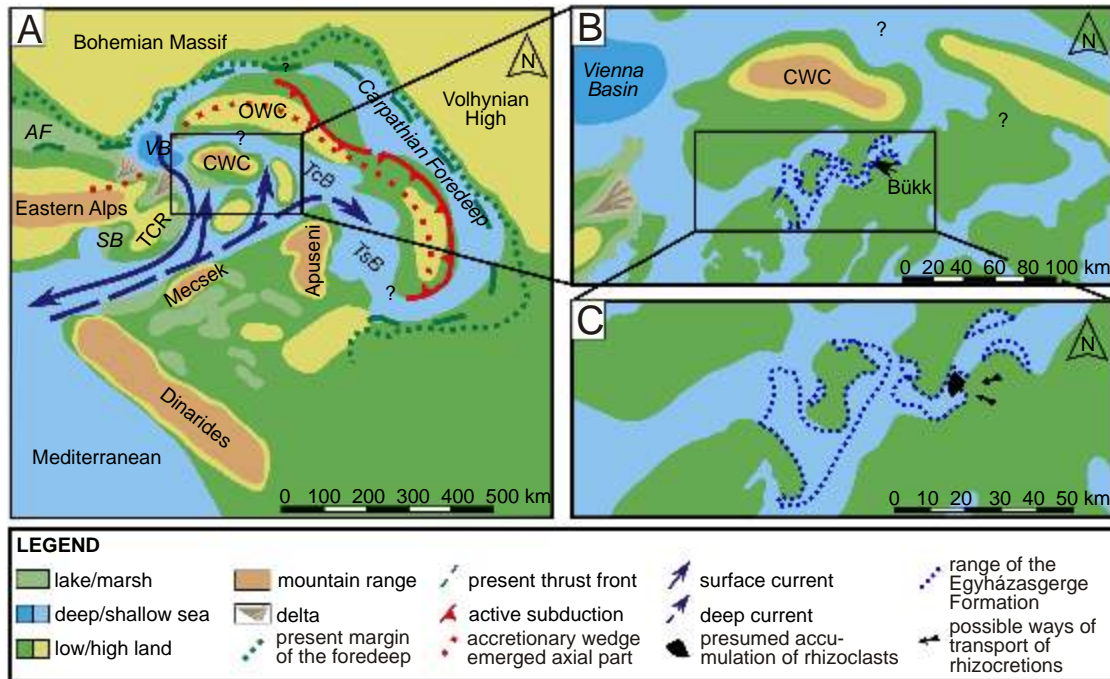


Fig. 16. Palaeogeography of the central Paratethys around the Early/Middle Miocene boundary: late Burdigalian–early Langhian

A – general map (AF – Alpine Foredeep, CWC – Central Western Carpathians, OWC – Outer Western Carpathians, SB – Styrian Basin, TcB – Transcarpathian Basin, TCR – Transdanubian High, TsB – Transylvanian Basin, VB – Vienna Basin); (?) assuming a brief marine connection (after Kova et al., 2017); **B** – palaeogeographic map of the north Hungarian Neogene Basin, including the distribution of the Egyházasgerge Formation (area encircled by the blue dashed line); **C** – area of inferred accumulation of the formations studied (based on Hámor, 2001; Püspöki et al., 2017)

salinity. A brackish environment has already been interpreted for the Egyházasgerge Formation based on the occurrence of *Congerina* and *Rzehakia* beds (Less et al., 2005). The presence of *Gyrolithes* corroborates this, since this trace fossil is common in brackish environments (Netto et al., 2007; Uchman and Hanken, 2013).

According to the palaeogeographic maps proposed for the area, the territory was occupied by a shallow water basin during the Karpatian (Fig. 16), where terrestrial and littoral sediments were deposited. The denuded area was presumably located between the Nógrád Basin and the Borsod Basin (Püspöki et al., 2017). In the latter, the Salgótarján Lignite Formation was deposited. This formation transits laterally to the Egyházasgerge Formation. The Salgótarján Lignite Formation represents a littoral facies in the vicinity of the study area, having sediments deposited in swampy and brackish water conditions (Püspöki, 2002). In exposures of the Salgótarján Lignite Formation, root remains and traces occur in the fine-grained deposits, particularly adjacent to coal seams (Dávid et al., 2006: fig. 4). Due to the transgressive nature of the littoral environment, erosional events could take place regularly. Thus, some rhizocretions may have been redeposited from this environment into the sedimentary basin of the Egyházasgerge Formation. However, it is not excluded that the rhizoclasts may derive from some older formation.

Ludvigson et al. (2013) wrote that rhizocretions composed of CaCO_3 originate in humid climates. It seems that the ferruginous-carbonate rhizocretions, such as some of those considered herein, originated in a more humid environment.

This is consistent with the lignite accumulations in the coeval Salgótarján Lignite Formation. The climate for the study area during the Karpatian was warm subtropical, and the land was vegetated by riparian forests, subtropical forests and hillside pine forests, with a contribution of tropical and temperate plants (Nagy, 1992). During the older Miocene, the climate in Hungary was tropical or subtropical, more or less humid (Nagy, 1990). The ferruginous rhizocretions from southwestern Poland (Fig. 10C) developed on living roots in a moderate climate with oceanic and continental influences. Concentric ferruginous rhizocretions form in the soils of Finland in a subarctic climate (Alhonen et al., 1975). This shows that the formation of rhizocretions containing a significant amount of iron is not strictly conditioned by the climate. However, iron must be mobilized and oxidized, usually under conditions of a fluctuating water table and oxygen levels (e.g., Bojanowski et al., 2016). Iron oxyhydroxides precipitate preferentially when groundwater passes through the redox boundary (Schwertmann and Murad, 1988; Hofmann, 1999; Yoshida et al., 2008), a condition likely to be more common in moderately and poorly drained soils. Furthermore, the formation of rhizocretions seems to be mediated by microbes (Alhonen et al., 1975; Yoshida et al., 2008).

Recognition of the proper nature of rhizoclasts can be important for interpretation of the palaeoenvironment of a source area. They point to a vegetated land in which roots penetrated into a fine-grained substrate, iron and calcium carbonate were mobilized, and the water table and oxygen levels fluctuated. They can be expected at least since the Middle Devonian, deposits of which contain ferruginous rhizocretions (Aleksseva,

2020). However, even Ordovician rhizocretions are possible, when clay-rich soils affected by ferruginization occurred (Retallack et al., 1985).

CONCLUSIONS

Disc-shaped and cylindrical structures from the brackish upper shoreface sands of the Egyházasgerge Formation (Miocene) in Hungary are fragmented and abraded calcareous and ferruginous rhizocretions, which were transported from a nearby landmass on which the Salgótarján Lignite Formation was deposited. These structures are termed rhizoclasts. They represent zombie biogenic structures inherited from another environment and playing other roles in a new, different environ-

ment. The presence of such structures in marine deposits can be considered as a proxy of nearby vegetated land, in which semi- or poorly-drained soils are developed, plant roots penetrate a fine-grained substrate where iron and calcium carbonate were mobilized, and the water table and oxygen levels fluctuated.

Acknowledgements. A.U. was supported by the Jagiellonian University. We are grateful M. Horváth who helped us collecting samples at the Bélapátfalva locality. We thank to M. Skiba, P. Wójcik-Tabol, B. Dziubińska, I. Brunarska and A. Wierzbicki (Kraków) for their help assistance in carrying out and interpreting of the laboratory analyses. The paper benefited from reviews by M. Verde (Montevideo) and M. Bojanowski (Warszawa).

REFERENCES

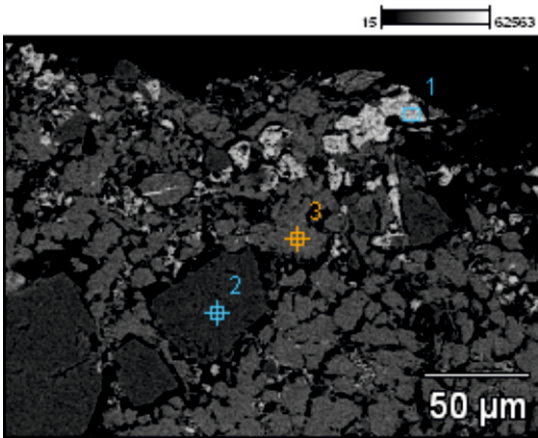
- Alekseeva, T.V., 2020. Rhizoliths in Devonian and Early Carboniferous palaeosols and their paleoecological interpretation. *Eurasian Soil Science*, **53**: 405–419. doi: 10.1134/S106422932004002X
- Alhonen, P., Koljonen, T., Lahermo, P., Uusinoka, R., 1975. Ferruginous concretions around root channels in clay and fine sand deposits. *Bulletin of the Geological Society of Finland*, **47**: 175–181. doi: 10.17741/bgsf/47.1-2.020
- Archibald, J.D., 1996. *Dinosaur Extinction and the End of an Era*. Columbia University Press.
- Barta, G., 2011. Secondary carbonates in loess-paleosol sequences: a general review. *Open Geosciences*, **3**: 129–146. doi: 10.2478/s13533-011-0013-7
- Becze-Deák, J., Langohr, R., Verrecchia, E., 1997. Small scale secondary CaCO₃ accumulations in selected sections of the European loess belt: morphological forms and potential for paleoenvironmental reconstruction. *Geoderma*, **76**: 221–252. doi: 10.1016/S0016-7061(96)00106-1
- Biernacka, J., Issmer, K., 1996. Micromorphological analysis of loess deposits from Klipcz, Western Pomerania (in Polish with English summary). *Przeegląd Geologiczny*, **44**: 43–48.
- Bojanowski, M.J., Jaroszewicz, E., Košir, A., Łoziński, M., Marynowski, L., Wysocka, A., Derkowski, A., 2016. Root-related rhodochrosite and concretionary siderite formation in oxygen-deficient conditions induced by a ground-water table rise. *Sedimentology*, **63**: 523–551. doi: 10.1111/sed.12227
- Bojanowski, M.J., Goryl, M., Kremer, B., Marciniak-Maliszewska, B., Marynowski, L., Rodó, J., 2020. Pedogenic siderites fossilizing Ediacaran soil microorganisms on the Baltica paleocontinent. *Geology*, **48**: 62–66. doi: 10.1130/g46746.1
- Canti, M., 1998. Origin of calcium carbonate granules found in buried soils and Quaternary deposits. *Boreas*, **27**: 275–288. doi: 10.1111/j.1502-3885.1998.tb01421.x
- Canti, M.G., Pearce, T.G., 2003. Morphology and dynamics of calcium carbonate granules produced by different earthworm species. *Pedobiologia*, **47**: 511–521. doi: 10.1078/0031-4056-00221
- Chesworth, W. (ed.), 2008. *Encyclopedia of Soil Science*. Springer, Dordrecht.
- Csontos, L., Vörös, A., 2004. Mesozoic plate tectonic reconstruction of the Carpathian region. *Palaeogeography, Palaeoclimatology, Palaeoecology*, **210**: 1–56. doi: 10.1016/j.palaeo.2004.02.033
- Dávid, Á., Püspöki, Z., Kónya, P., Vincze, L., Kozák, M., McIntosh, R.W., 2006. Sedimentology, paleoichnology and sequence stratigraphy of a Karpathian sandy facies (Salgótarján Lignite Formation, N Hungary). *Geologica Carpathica*, **57**: 279–94.
- Dávid, Á., Kovács, B., Fodor, R., 2008. Bioerosion in the shells of Early Miocene Balanidae (Bükk Mountains, Hungary). In: Abstracts of the 6th. International Bioerosion Workshop Salt Lake City (UT), USA, July13–20th. Salt Lake City.
- Dávid, Á., Uchman, A., Fodor, R., 2015. *Dactyloidites peniculus* from the Early Miocene of Hungary. In: SLIC 2015, Third Latin American Symposium on Ichnology, Abstracts and Intra-Symposium Fieldtrip Guide (eds. M. Verde and G. Roland): 38. Colonia del Sacramento, Uruguay.
- Durand, N., Monger, H.C., Canti, M.G., 2010. Calcium carbonate features. In: Interpretation of Micromorphological Features of Soils and Regoliths (eds. G. Stoops, V. Marcelino and F. Mees): 149–193. Elsevier B.V.
- Gocke, M., Wiesenberg, G.L.B., Löscher, M., Pustovoytov, K., Kuzyakov, Y., 2009. Rhizoliths in loess – determination of the origin using organic geochemical approaches. EGU General Assembly 2009, held 19–24 April, 2009 in Vienna, Austria: 7861. <http://meetings.copernicus.org/egu2009>
- Gocke, M., Kuzyakov, Y., Wiesenberg, G.L.B., 2010. Rhizoliths in loess – evidence for post-sedimentary incorporation of root-derived organic matter in terrestrial sediments as assessed from molecular proxies. *Organic Geochemistry*, **41**: 1198–1206. doi: 10.1016/j.orggeochem.2010.08.001
- Gocke, M., Pustovoytov, K., Kühn, K.P., Wiesenberg, G.L.B., Löscher, M., Kuzyakov, Y., 2011. Carbonate rhizoliths in loess and their implications for paleoenvironmental reconstruction revealed by isotopic composition: ¹³C, ¹⁴C. *Chemical Geology*, **283**: 251–260. doi: 10.1016/j.chemgeo.2011.01.022
- Gyalog, L. ed., 1996. A földtani térképek jelkulcsa és a rétegtani egységek rövid leírása (in Hungarian). Geological Institute of Hungary, Budapest.
- Hámor, G., 2001. Miocene palaeogeography of the Karpathian Basin: interpretation for the Miocene palaeogeographic and facies maps of the Karpathian Basin (in Hungarian). Geological Institute of Hungary, Budapest.
- Hofmann, B.A., 1999. Geochemistry of natural redox fronts – a review. Technical Report Nagra 99-05. National Cooperative for the Disposal of Radioactive Waste, Wettingen: 142.
- Klappa, C.F., 1980. Rhizoliths in terrestrial carbonates: classification, recognition, genesis and significance. *Sedimentology*, **27**: 613–629. doi: 10.1111/j.1365-3091.1980.tb01651.x
- Kovács, M., Hudáková, N., Halásóvá, E., Kováčová, M., Holcová, K., Oszczytko-Clowes, M., Báldi, K., Less, G., Nagymarosy, A., Ruman, R., Klujár, T., Jamrich, M., 2017. The Central Paratethys palaeoceanography: a water circulation model ba-

- sed on microfossil proxies, climate, and changes of depositional environment. *Acta Geologica Slovaca*, **9**: 75–114.
- Ł **cka, B., Łanczont, M., Komar, M., Madeyska, T., 2008.** Stable isotope composition of carbonates in loess at the Carpathian margin (SE Poland). *Studia Quaternaria*, **25**: 3–21.
- Ł **cka, B., Łanczont, M., Madeyska, T., 2009.** Oxygen and carbon stable isotope composition of authigenic carbonates in loess sequences from the Carpathian margin and Podolia, as a palaeoclimatic record. *Quaternary International*, **198**: 136–151. doi.org/10.1016/j.quaint.2008.02.001
- Lane, A., Janis, C.M., Sepkoski, J.J., Jr., 2005.** Estimating paleodiversities: a test of the taxic and phylogenetic methods. *Paleobiology*, **31**: 21–34.
- Laskowska-Wysocza ska, W., 1971.** Quaternary stratigraphy and palaeogeomorphology of the Sandomierz Lowland and the Foreland of the Middle Carpathians, Poland (in Polish with English summary). *Studia Geologica Polonica*, **34**: 1–109.
- Laskowska-Wysocza ska, W., 1995.** Neotectonic and glacial control on geomorphic development of middle and eastern parts of the Sandomierz Basin and the Carpathian margin. *Folia Quaternaria*, **66**: 105–122.
- Lee, M.R., Hodson, M.E., Langworthy, G., 2008.** Earthworms produced granules of intricately zoned calcite. *Geology*, **36**: 943–946. doi: 10.1130/G25106A.1
- Less, G., Kovács, S., Pelikán P. (Ed.), Pentelényi, L., Sásdi, L., 2005.** Geology of the Bükk Mountains. Explanatory Book to the Geological Map of the Bükk Mountains (1:50 000). Magyar Állami Földtani Intézet kiadványa, Budapest.
- Löwemark, L., Zheng, Y.C., Das, S., Yeh, C.P., Chen, T.T., 2016.** A peculiar reworking of *Ophiomorpha* shafts in the Miocene Nangang Formation, Taiwan. *Geodinamica Acta*, **28**: 71–85. doi: 10.1080/09853111.2015.1035208
- Ludvigson, G.A., González, L.A., Fowle, D.A., Roberts, J.A., Driese, S.G., Villarreal, M.A., Smith, J.J., Suarez, M.B., 2013.** Paleoclimatic applications and modern process studies of pedogenic siderite. *SEPM Special Publication*, **44**: 79–87. doi:10.2110/sepm.sp.104.01
- Metodiev, L., Petrova, S., Dochev, D., Dimova, L., 2022.** Interfluvial waterlogged palaeosols preserved within offshore shales? Preliminary data from the Aalenian of West Bulgaria. In: XXII International Congress of the CBGA, Plovdiv, Bulgaria, 7–11 September 2022, Abstracts (eds. I. Peycheva, A. Lazarova, G. Grančovski, R. Ivanova, I. Lakova and L. Metodiev): 52. *Geologica Balcanica*, Plovdiv.
- Nagy, E., 1990.** Climatic changes in the Hungarian Miocene. Review of Palaeobotany and Palynology, **65**: 71–74. doi.org/10.1016/0034-6667(90)90057-P
- Nagy, E., 1992.** A comprehensive study of Neogene sporomorphs in Hungary (in Hungarian with English summary). *Geologica Hungarica, Series Palaeontologica*, **53**: 1–379.
- Nanzyo, M., Kanno, H., 2018.** Inorganic Constituents in Soil: Basics and Visuals. Springer Open, Singapore. doi: 10.1007/978-981-13-1214-4
- Netto, R.G., Buatois, L.A., Mángano, M., Balistieri, P., 2007.** *Gyrolithes* as a multipurpose burrow: an ethological approach. *Revista Brasileira de Paleontologia*, **10**: 157–168. doi: 10.4072/rbp.2007.3.03
- Owen, R.A., Owen, R.B., Renault, R.W., Scott, J.J., Jones, B., Ashley, G.M., 2008.** Mineralogy and origin of rhizoliths on the margins of saline, alkaline Lake Bogoria, Kenya Rift Valley. *Sedimentary Geology*, **203**: 143–163. doi.org/10.1016/j.sedgeo.2007.11.007
- Pedrol de Freitas, G., Francischini, H., Tapajós de Souza Tâmega, F., Spotorno-Oliveira, P., Dentzien-Dias, P., 2020.** On ex situ *Ophiomorpha* and other burrow fragments from the Rio Grande do Sul Coastal Plain, Brazil: paleobiological and taphonomic remarks. *Journal of Paleontology*, **94**: 1148–1164. doi: 10.1017/jpa.2020.29
- Pemberton, G.S., Spila, M., Pulham, A.J., Saunders, T., MacEachern, J.A., Robbins, D., Sinclair, I.K., 2001.** Ichnology and sedimentology of shallow to marginal marine systems: Ben Nevis and Avalon Reservoirs, Jeanne D'Arc Basin. Geological Association of Canada, Short Course Notes, 15.
- Püspöki, Z., 2002.** A Tardonai-dombság miocén medencefejlése az üledékes szekvenciák fácies- és rétegtani adatainak tükrében (in Hungarian). Ph.D. Thesis, University of Debrecen.
- Püspöki, Z., Hámor-Vidó, M., Pummer, T., Sári, K., Lendvay, P., Selmeczi, I., Detzky, G., Gúthy, T., Kiss, J., Kovács, Z., Práfkalvi, P., McIntosh, R.W., Buday-Bódi, E., Báldi, K., Markos, G., 2017.** A sequence stratigraphic investigation of a Miocene formation supported by coal seam quality parameters – Central Paratethys, N-Hungary. *International Journal of Coal Geology*, **179**: 196–210. doi: 10.1016/j.coal.2017.05.016
- Radócz, G., 1977.** Paleolithic data from the beach sands of the Helvetic sequence at Bélapátfalva, NE Hungary (in Hungarian with English summary). *A Magyar Állami Földtani Intézet Évi Jelentése*, **1975**: 83–95.
- Renaut, R.W., 1993.** Zeolitic diagenesis of late Quaternary fluvio-lacustrine sediments and associated calcareous formation in the Lake Bogoria Basin, Kenya Rift Valley. *Sedimentology*, **40**: 271–301. doi.org/10.1111/j.1365-3091.1993.tb01764.x
- Retallack, G.J., Catt, J.A., Chaloner, W.G., 1985.** Fossil soils as grounds for interpreting the advent of large plants and animals on land. *Philosophical Transactions of the Royal Society, London*, **B309**: 105–142. doi.org/10.1098/rstb.1985.0074
- Schwertmann, U., Murad, E., 1988.** The nature of an iron oxide – organic iron association in peaty environment. *Clay Minerals*, **23**: 291–299. doi.org/10.1180/claymin.1988.023.3.06
- Sharkan, N., Achyuthan, H., 2007.** Genesis of calcic and petrocalcic horizons from Coimbatore, Tamil Nadu: micromorphology and geochemical studies. *Quaternary International*, **175**: 140–154. doi.org/10.1016/j.quaint.2007.05.017
- Sieglitz, R.D., Van Horn, R.G., 1982.** Post-Pleistocene development of root-shaped ferruginous concretions. *Ohio Journal of Science*, **82**: 14–18.
- Taylor, A.M., Goldring, R., 1993.** Description and analysis of bioturbation and ichnofabric. *Journal of the Geological Society*, **150**: 141–148. doi.org/10.1144/gsjgs.150.1.014
- Uchman, A., Hanken, N.-M., 2013.** The new trace fossil *Gyrolithes lorcaensis* isp. n. from the Miocene of SE Spain and a critical review of the *Gyrolithes* ichnospecies. *Stratigraphy and Geological Correlation*, **21**: 72–84. doi: 10.1134/S0869593813030088
- Vepreskas, M.J., Lindbo, D.L., Stolt, M.H., 2018.** Redoximorphic features. In: Interpretation of Micromorphological Features of Soils and Regoliths (eds. G. Stoops, V. Marcelino and F. Mees): 424–445. Elsevier, Amsterdam.
- Versteegh, E.A.A., Black, S., Canti, M.G., Hodson, M.E., 2013.** Earthworm-produced calcite granules: a new terrestrial palaeothermometer? *Geochimica et Cosmochimica Acta*, **123**: 351–357. doi: 10.1016/j.gca.2013.06.020
- Yoshida, H., Yamamoto, K., Murakami, Y., Katsuta, N., Hayashi, T., Naganuma, T., 2008.** The development of Fe-nodules surrounding biological material mediated by microorganisms. *Environmental Geology*, **55**: 1363–1374. doi: 10.1007/s00254-007-1087-x

APPENDIX 1

EDS analysis of three mineral grains in a thin-section from a spindle rhizoclast, Bélapátfalva pit

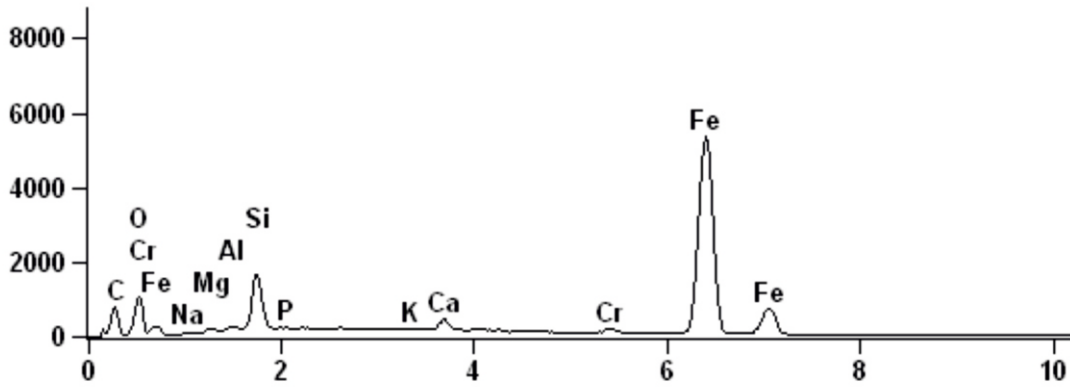
Bela-10(1)



This filed view is in Fig. 10A
Accelerating Voltage: 20.0 kV

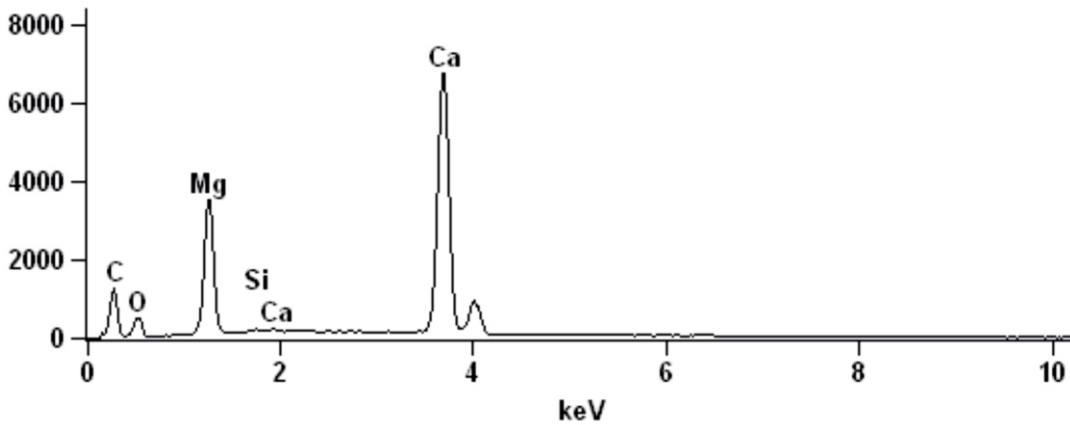
Full scale counts: 5363

Bela-10(1)_pt1



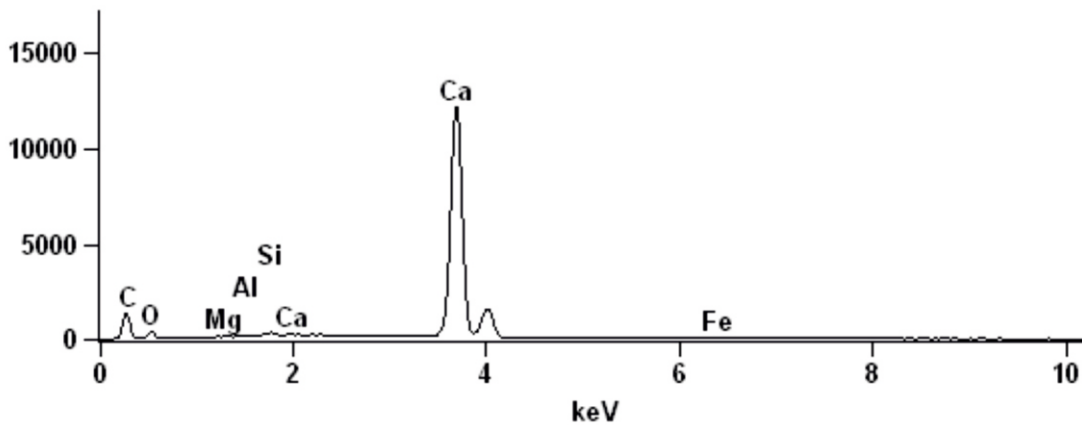
Full scale counts: 6743

Bela-10(1)_pt2



Full scale counts: 12128

Bela-10(1)_pt3



Net Counts

	O-K	Na-K	Mg-K	Al-K	Si-K	P-K	K-K	Ca-K	Cr-K	Fe-K
<i>Bela-10(1)_pt1</i>	6417	295	513	748	14902	343	514	3418	1413	90191
<i>Bela-10(1)_pt2</i>	3858		30542		364			91420		
<i>Bela-10(1)_pt3</i>	2605		287	354	768			166451		747

Net Counts Error (+/- 1 Sigma)

	O-K	Na-K	Mg-K	Al-K	Si-K	P-K	K-K	Ca-K	Cr-K	Fe-K
<i>Bela-10(1)_pt1</i>	+/-151	+/-43	+/-55	+/-75	+/-192	+/-94	+/-89	+/-197	+/-96	+/-526
<i>Bela-10(1)_pt2</i>	+/-83		+/-212		+/-68			+/-540		
<i>Bela-10(1)_pt3</i>	+/-75		+/-57	+/-70	+/-131			+/-808		+/-85

Weight %

	O-K	Na-K	Mg-K	Al-K	Si-K	P-K	K-K	Ca-K	Cr-K	Fe-K
<i>Bela-10(1)_pt1</i>	32.875	0.39	0.38	0.36	5.28	0.12	0.15	1.01	0.59	58.85
<i>Bela-10(1)_pt2</i>	32.565		21.21		0.19			46.05		
<i>Bela-10(1)_pt3</i>	28.805		0.20	0.17	0.29			69.76		0.79

Weight % Error (+/- 1 Sigma)

	O-K	Na-K	Mg-K	Al-K	Si-K	P-K	K-K	Ca-K	Cr-K	Fe-K
<i>Bela-10(1)_pt1</i>	+/-0.77	+/-0.06	+/-0.04	+/-0.04	+/-0.07	+/-0.03	+/-0.03	+/-0.06	+/-0.04	+/-0.34
<i>Bela-10(1)_pt2</i>	+/-0.70		+/-0.15		+/-0.04			+/-0.27		
<i>Bela-10(1)_pt3</i>	+/-0.83		+/-0.04	+/-0.03	+/-0.05			+/-0.34		+/-0.09

Atom %

	O-K	Na-K	Mg-K	Al-K	Si-K	P-K	K-K	Ca-K	Cr-K	Fe-K
<i>Bela-10(1)_pt1</i>	60.67	0.51	0.46	0.39	5.55	0.11	0.11	0.75	0.34	31.12
<i>Bela-10(1)_pt2</i>	50.08		21.47		0.17			28.28		
<i>Bela-10(1)_pt3</i>	50.29		0.23	0.17	0.29			48.63		0.40

Atom % Error (+/- 1 Sigma)

	O-K	Na-K	Mg-K	Al-K	Si-K	P-K	K-K	Ca-K	Cr-K	Fe-K
<i>Bela-10(1)_pt1</i>	+/-1.43	+/-0.07	+/-0.05	+/-0.04	+/-0.07	+/-0.03	+/-0.02	+/-0.04	+/-0.02	+/-0.18
<i>Bela-10(1)_pt2</i>	+/-1.08		+/-0.15		+/-0.03			+/-0.17		
<i>Bela-10(1)_pt3</i>	+/-1.45		+/-0.05	+/-0.03	+/-0.05			+/-0.24		+/-0.04

Formula

	O-K	Na-K	Mg-K	Al-K	Si-K	P-K	K-K	Ca-K	Cr-K	Fe-K
<i>Bela-10(1)_pt1</i>		Na2O	MgO	Al2O3	SiO2	P2O5	K2O	CaO	Cr2O3	Fe2O3
<i>Bela-10(1)_pt2</i>			MgO		SiO2			CaO		
<i>Bela-10(1)_pt3</i>			MgO	Al2O3	SiO2			CaO		Fe2O3

Compound %

		Na2O	MgO	Al2O3	SiO2	P2O5	K2O	CaO	Cr2O3	Fe2O3
<i>Bela-10(1)_pt1</i>	0.00	0.53	0.63	0.67	11.29	0.27	0.18	1.42	0.87	84.14
<i>Bela-10(1)_pt2</i>	0.00		35.17		0.41			64.43		
<i>Bela-10(1)_pt3</i>	0.00		0.33	0.32	0.62			97.60		1.13

Cations

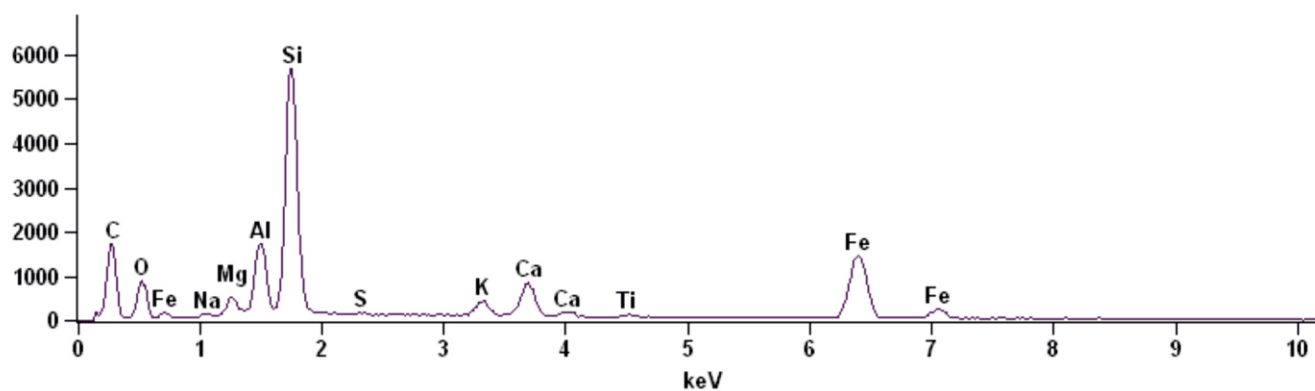
	O-K	Na-K	Mg-K	Al-K	Si-K	P-K	K-K	Ca-K	Cr-K	Fe-K
<i>Bela-10(1)_pt1</i>	0.00	0.20	0.18	0.15	2.20	0.04	0.04	0.29	0.13	12.31
<i>Bela-10(1)_pt2</i>	0.00		10.29		0.08			13.55		
<i>Bela-10(1)_pt3</i>	0.00		0.11	0.08	0.14			23.21		0.19

APPENDIX 2

Net results of EDS analysis of a large surface illustrated in Fig. 11A in a spindle-shaped rhizoclast, which less calcareous and more ferruginous than in A, Bélápátfalva pit

Full scale counts: 5675

Bela-2(1)



Quantitative Results for: Bela-2(1)

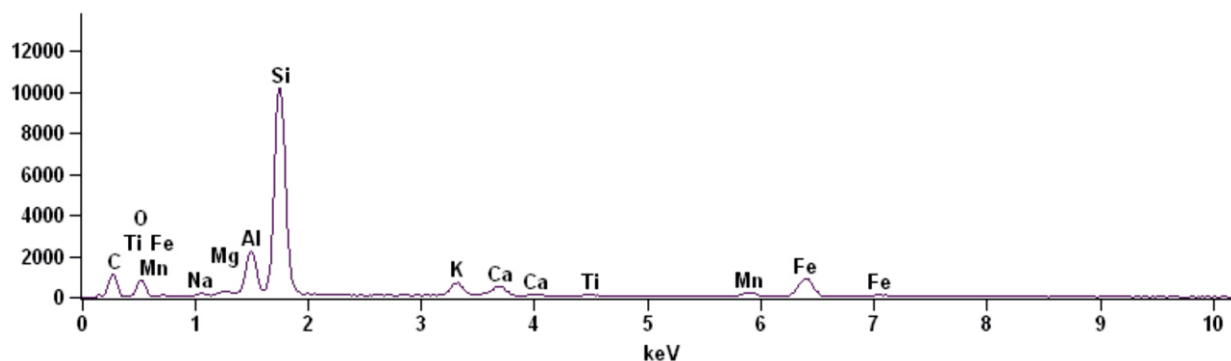
Element Line	Net Counts	Net Counts Error	Weight %	Weight % Error	Atom %	Atom % Error	Formula	Compnd %	# Cations
O K	6569	+/- 127	42.84S	---	62.31	+/- 1.20	---	---	---
Na K	401	+/- 58	0.43	+/- 0.06	0.43	+/- 0.06	Na ₂ O	0.58	0.166
Mg K	3019	+/- 131	1.85	+/- 0.08	1.77	+/- 0.08	MgO	3.07	0.684
Al K	14958	+/- 237	6.42	+/- 0.10	5.54	+/- 0.09	Al ₂ O ₃	12.13	2.133
Si K	57133	+/- 373	21.32	+/- 0.14	17.66	+/- 0.12	SiO ₂	45.61	6.804
S K	387	+/- 76	0.15	+/- 0.03	0.11	+/- 0.02	SO ₃	0.37	0.041
K K	3720	+/- 187	1.41	+/- 0.07	0.84	+/- 0.04	K ₂ O	1.69	0.322
Ca K	9954	+/- 224	3.93	+/- 0.09	2.28	+/- 0.05	CaO	5.50	0.879
Ti K	691	+/- 129	0.36	+/- 0.07	0.18	+/- 0.03	TiO ₂	0.60	0.068
Fe K	25190	+/- 307	21.30	+/- 0.26	8.88	+/- 0.11	Fe ₂ O ₃	30.45	3.419
Total			100.00		100.00			100.00	14.515

APPENDIX 3

Net results of EDS analysis of a large surface illustrated in Fig. 14C in a breaking surface of a rhizcretion from the Quaternary deposits of SE Poland (locality between Husów and Handzlówka)

Full scale counts: 10186

Gaj-1(4)



Quantitative Results for: Gaj-1(4)

Element Line	Net Counts	Net Counts Error	Weight %	Weight % Error	Atom %	Atom % Error	Formula	Compnd %	# Cations
O K	6098	+/- 115	46.235	---	63.33	+/- 1.19	---	---	---
Na K	1081	+/- 86	0.82	+/- 0.06	0.78	+/- 0.06	Na ₂ O	1.10	0.295
Mg K	1603	+/- 127	0.72	+/- 0.06	0.65	+/- 0.05	MgO	1.19	0.245
Al K	19012	+/- 262	5.97	+/- 0.08	4.85	+/- 0.07	Al ₂ O ₃	11.28	1.837
Si K	105212	+/- 528	29.62	+/- 0.15	23.11	+/- 0.12	SiO ₂	63.36	8.759
K K	7312	+/- 213	2.35	+/- 0.07	1.32	+/- 0.04	K ₂ O	2.83	0.499
Ca K	5883	+/- 207	1.98	+/- 0.07	1.08	+/- 0.04	CaO	2.77	0.410
Ti K	1169	+/- 142	0.52	+/- 0.06	0.24	+/- 0.03	TiO ₂	0.87	0.090
Mn K	2864	+/- 108	1.92	+/- 0.07	0.77	+/- 0.03	MnO	2.48	0.291
Fe K	13950	+/- 264	9.88	+/- 0.19	3.88	+/- 0.07	Fe ₂ O ₃	14.13	1.470
Total			100.00		100.00			100.00	13.895

APPENDIX 4

XRD spectograms of a part of the spindle-shaped rhizoclast from part B of this Supplementary material, and a rhizocretion from the Quaternary deposits of SE Poland (locality between Husów and Handzlówka)

